An imbricate midcrustal suture zone: The Mojave-Yavapai Province boundary in Grand Canyon, Arizona

Mark E. Holland[1,†], K.E. Karlstrom[1], M.F. Doe[2], G.E. Gehrels[3], M. Pecha[3], O.P. Shufeldt[4], G. Begg[5,6], W.L. Griffin[6], and Elena Belousova[6]

[1]*Department of Earth and Planetary Sciences, University of New Mexico, Northrop Hall, 221 Yale Boulevard NE, Albuquerque, New Mexico 87106, USA*

[2]*Department of Geology and Geologic Engineering, Colorado School of Mines, Golden, Colorado 80401, USA*

[3]*Arizona LaserChron Center, Department of Geosciences, University of Arizona, Tucson, Arizona 85721, USA*

[4]*Rio Tinto Iron Ore, Perth, WA 6000, Australia*

[5]*Minerals Targeting International PL, West Perth, WA 6005, Australia*

[6]*Australian Research Council Centre of Excellence for Core to Crust Fluid Systems/GEMOC, Macquarie University, Sydney, NSW 2109, Australia*

ABSTRACT

The Paleoproterozoic Mojave and Yavapai crustal provinces in southwestern Laurentia contain evolved and juvenile crust, respectively, but the nature of the province boundary remains uncertain. 1.78–1.35 Ga crystalline basement rocks of the Mojave Province preserve an evolved isotopic signature reflecting an Archean crustal component in several isotopic systems (Nd, Pb, Hf). However, no Archean rocks have been found, and hence the origin and tectonic significance of this Archean component are also unclear. This paper analyzes the U-Pb age and Hf isotopic composition of zircons from both the oldest granodiorite plutons (1.84–1.71 Ga) and the oldest metasedimentary rocks (1.75 Ga Vishnu Schist) across a 180-km-long cross-strike transect in Grand Canyon. This transect crosses the Crystal shear zone, which has been proposed as the location of a suture separating the provinces. Our results show that the characteristically bimodal population of detrital zircons in the Vishnu Schist (2.5 Ga and 1.8 Ga modes) yields mixed $\varepsilon_{Hf(t)}$ values, primarily between +5 to –5, that are uniform across the transect. Another new finding is that the 1.84 Ga Elves Chasm pluton, on which the Vishnu Schist was deposited, yields juvenile $\varepsilon_{Hf(t)}$ values of +5 to +12 and was not the dominant source for the ca. 1.85 Ga peak in the 1.75 Ga Vishnu Schist. Instead, the Vishnu Schist was derived from an Archean craton mixed with intermediate to evolved 1.85 Ga crust. Metasediments show no evidence in support of the proposed suture. Paradoxically, plutons east and west of the Crystal shear zone do support models for a crustal suture. Plutons east of the Crystal shear zone dated at 1.74–1.71 Ga yield juvenile $\varepsilon_{Hf(t)}$ values of +5 to +12 that are characteristic of the Yavapai Province. Plutons west of the Crystal shear zone show juvenile to evolved Paleoproterozoic grains ($\varepsilon_{Hf(t)}$ of –5 to +10) as well as xenocrystic Archean and 1.85 Ga grains ($\varepsilon_{Hf(t)}$ of –12 to +10). These data support the proposition that the Crystal shear zone marks a sharp boundary between the Mojave and Yavapai crustal provinces. However, the overlapping Vishnu Schist suggests a more complicated crustal architecture. The depositional setting of the Vishnu Schist remains unclear; however, we interpret the ultimate geometry of the transect to reflect an ~200-km-wide middle-crustal duplex system in which the 1.75 Ga Vishnu Schist was deposited across both Mojave and Yavapai crust. This system was subsequently imbricated in an accretionary complex. The ultimate architecture is of a distributed boundary with slivers of plutons that carry the isotopic signature of their respective provinces imbricated within metasediments.

INTRODUCTION

The core of the North American continent was assembled by collision of Archean cratons during the 1.83–1.80 Ga Trans-Hudson orogeny (Hoffman, 1988; Corrigan et al., 2005, 2009) followed by progressive southward (present coordinates) addition of lithosphere in accretionary orogens of southwestern Laurentia (Karlstrom and Bowring, 1988; Windley, 2003) beginning ca. 1.8 Ga and culminating with the Grenville orogeny and assembly of Rodinia (e.g., Whitmeyer and Karlstrom, 2007). In this model, southern Laurentia is an important field laboratory for studies of continent formation processes because it has been interpreted as an amalgamation of dominantly juvenile Paleoproterozoic terranes that were added to the Archean and 1.8 Ga nucleus (Fig. 1, inset; DePaolo, 1981; Hoffman, 1988; Karlstrom and Bowring, 1988; Bowring and Karlstrom, 1990; Duebendorfer, 2007). Further, this region may represent one of the largest additions of juvenile continental crust in Earth history (Reymer and Schubert, 1986). Alternatively, new models suggest that many orogens previously thought to be predominantly accretionary can contain hybridized and metasomatized lithosphere where cryptic substrates of older lower crust and mantle lithosphere underlie younger crust (Begg et al., 2007, 2009a, 2009b; Griffin et al., 2008, 2011; Belousova et al., 2009, 2010).

The Mojave Province of southwestern Laurentia (Fig. 1) has long been known to include older crustal material (Bennett and DePaolo, 1987; Wooden and Miller, 1990; Chamberlain and Bowring, 1990; Wooden and DeWitt, 1991; Ramo and Calzia, 1998; Ilg et al., 1996; Hawkins et al., 1996; Iriondo et al., 2004; Barth et al., 2000, 2009; Wooden et al., 2012), but the age, origin, and distribution of this material remain uncertain. A parallel debate has involved the boundary between the Mojave Province and the Yavapai Province, which contains 1.8–1.7 Ga juvenile crust (Wooden and DeWitt, 1991; Karlstrom and Bowring, 1993; Bennett and DePaolo, 1987; Duebendorfer et al., 2006). Previous models of the nature of the Mojave

†medwardholland89@gmail.com

GSA Bulletin; September/October 2015; v. 127; no. 9/10; p. 1391–1410; doi: 10.1130/B31232.1; 15 figures; 1 table; Data Repository item 2015158; published online 15 April 2015.

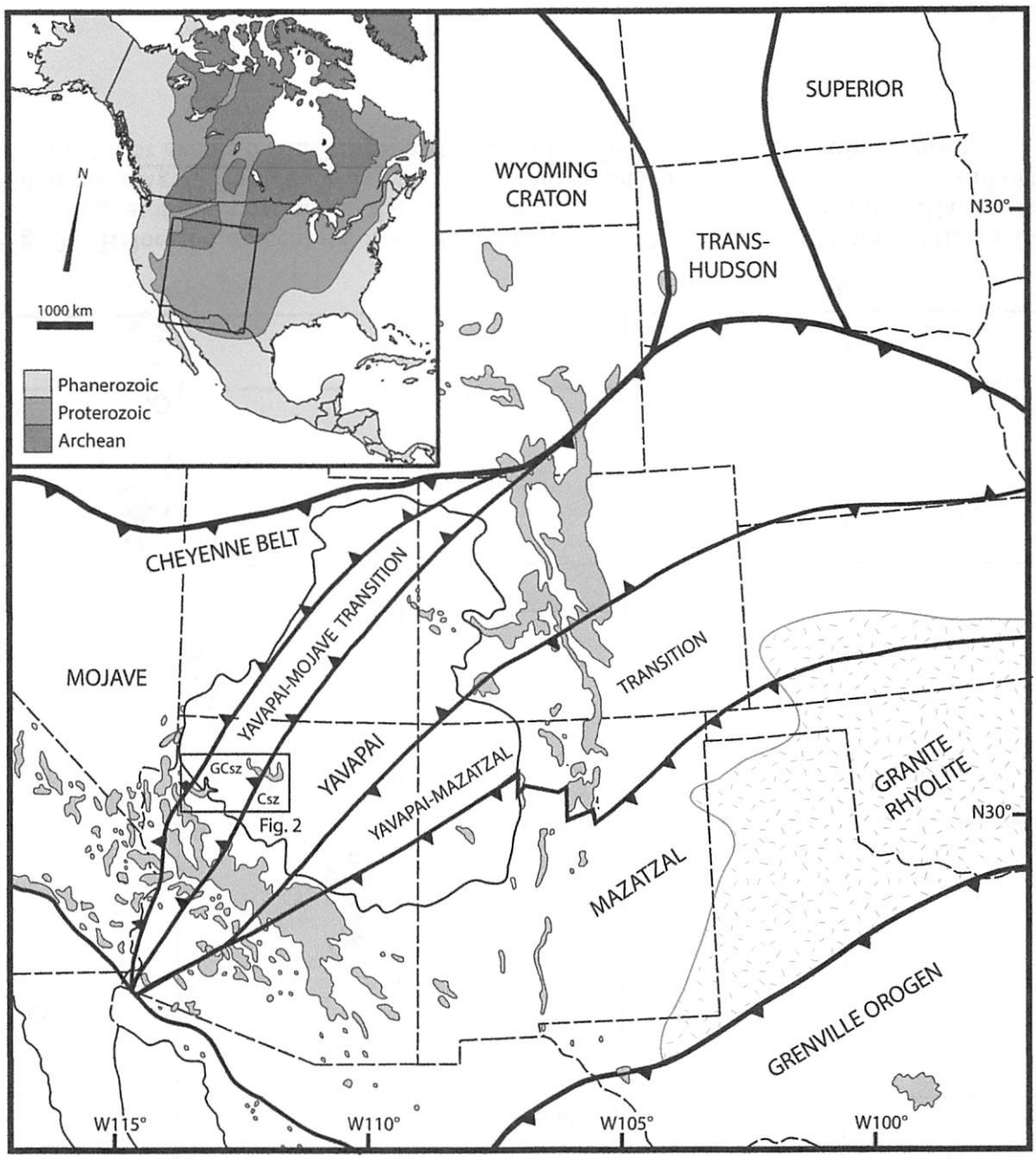

Figure 1. Regional map of Proterozoic provinces of western Laurentia modified after Karlstrom et al. (2004). Outcrops of Proterozoic rocks are shown in gray. Box shows location of Figure 2. Csz—Crystal shear zone, GCsz—Gneiss Canyon shear zone.

Province's inherited signature and the Mojave-Yavapai boundary include: (1) subducted Archean detritus as the source of the evolved isotopic signature of the Mojave Province, with inherited signature decreasing with distance from the Archean Wyoming Province (Bennett and DePaolo, 1987; Ramo and Calzia, 1998), (2) an ~75-km-wide boundary zone defined by whole-rock and feldspar Pb isotopic data that was interpreted to be the result of post–1.73 Ga modification of the Mojave-Yavapai boundary by deformation and plutonism after the provinces were tectonically juxtaposed (Wooden and DeWitt, 1991), (3) a distributed tectonic suture centered at the Crystal shear zone in Grand Canyon (Ilg et al., 1996; Hawkins et al., 1996) that extends ~130 km to the Gneiss Canyon shear zone in western Grand Canyon (Karlstrom et al., 2003), (4) a wide isotopically mixed zone resulting from rifting and hybridization of older crust (Duebendorfer et al., 2006), and (5) the presence of Archean crust in middle- to lower-crustal subcrops of the Mojave Province that contributed detritus to the Vishnu Schist (Shufeldt et al., 2010).

A recent detrital zircon study was conducted on the Vishnu Schist in the Grand Canyon, which spans over 30 km on both sides of the proposed Crystal suture zone (Shufeldt et al., 2010). Laser-ablation–multicollector–inductively

coupled plasma–mass spectrometry (LA-MC-ICP-MS) analysis of >1000 grains separated from 12 spatially distributed samples along a 180-km-long cross-strike transect revealed a uniform bimodal detrital zircon age population with peaks at 1.8 Ga and 2.5 Ga. This surprising result lead Shufeldt et al. (2010) to conclude that: (1) any collision of Yavapai crust with Mojave crust either predated or was synchronous with Vishnu deposition at 1.75 Ga because the turbidite succession overlaps the proposed crustal boundary at the Crystal shear zone; (2) these sediments were not derived from juvenile terranes, as only 13% were 1.75 Ga grains; (3) the ca. 1.85 Ga peak in the metasediments was derived from the underlying 1.84 Ga Elves Chasm gneiss; and (4) an older Mojave crustal substrate contributed detritus to the Vishnu Schist.

The purpose of this paper is to present new Hf and U-Pb data from the oldest rocks in the Grand Canyon and use a synthesis of all available age and isotopic data to test models that explain the nature of the Mojave-Yavapai boundary. The goal is to resolve the nature of the Crystal shear zone by comparing the U-Pb and Hf isotopic composition of zircons from the Vishnu metaturbidite with those from plutons that intrude on both sides of the Crystal shear zone. This methodology will test the hypotheses of Hawkins et al. (1996) and Shufeldt et al. (2010) that the Crystal shear zone represents a Mojave-Yavapai crustal boundary, and that there exists an older crustal substrate in the Mojave Province. The excellent exposure of a 180-km-long cross-strike basement transect, the uniform detrital zircon population of the Vishnu Schist, and the well-described structural, geochronologic, and thermobarometric history of the Granite Gorges make the Grand Canyon an ideal field locality for exploring and resolving the timing and character of the Mojave-Yavapai crustal boundary.

New data include paired U-Pb and Hf isotopic analyses of 187 detrital zircons from the Vishnu Schist, and 233 igneous zircons from 10 plutons that intrude the Vishnu Schist, from east to west across the entire transect. Our approach of applying paired U-Pb dating and Hf isotopic analysis to the oldest metasedimentary rocks and the oldest plutons in the orogen provides a powerful data set with which to constrain the earliest evolution of the Mojave and Yavapai Provinces. These data provide both "top-down" and "bottom-up" views of the crust in the region. U-Pb and Hf composition of zircons collected from metasedimentary rocks provide information about the age and chemical maturity of crust exposed in the provenance region during the time of deposition. Conversely, the U-Pb and Hf compositions of zircons separated from intrusive lithologies provide information about the character of their lower-crustal melt source regions. The concept of using plutons as probes of the lower-crustal melt reservoirs has been applied to many orogens. Examples include the North American Cordillera (Farmer and DePaolo, 1983; Samson et al., 1989, 1991; Friedman et al., 1995), the Variscan (Finger, 1997) and Alpine orogens (Kohút and Nabelek, 2008), and the Central Asian orogenic belt (Jahn et al., 2000; Kovalenko et al., 2004). Hf isotopes of plutonic zircons have been used to evaluate the participation of juvenile versus evolved crust in Proterozoic terranes (Andersen et al., 2002), and to discern terrane boundaries and infer crustal architecture (Cecil et al., 2011; Foster et al., 2012).

GEOLOGIC BACKGROUND

Basement rocks are exposed from river mile (RM, measured downstream from Lees Ferry) 78–260 within the Upper Granite Gorge (RM 78–116) and Lower Granite Gorge (RM 208–260) segments. The Upper Granite Gorge is characterized by a block-type architecture, consisting of six ~10-km-scale tectonic blocks bounded by five discrete high-strain zones, the deformational and metamorphic character of which has been studied previously (Ilg et al., 1996; Hawkins et al., 1996; Karlstrom et al., 2003; Dumond et al., 2007). These six blocks, from east to west, are the Mineral Canyon, Clear Creek, Trinity Creek, Topaz Canyon, Tuna Creek, and Walthenberg Canyon blocks. Two blocks are sampled in the Lower Granite Gorge: the Travertine Grotto and Spencer Canyon blocks, separated by the Gneiss Canyon shear zone (Karlstrom et al., 2003). These eight blocks all contain Vishnu Schist, and they share a similar 1.75–1.69 Ga tectonic history, as described later herein.

Upper Granite Gorge contains about half supracrustal and half plutonic rocks (Fig. 2). The supracrustal Granite Gorge metamorphic suite is composed of three intimately interlayered but mappable units: the 1740 ± 2 Ma Rama Schist, the 1750 ± 1 Ma Brahma Schist, and the Vishnu Schist. These felsic and mafic metavolcanic, and metaturbidite units, respectively, were interpreted to represent juvenile marine volcanic-arc rocks (Hawkins et al., 1996; Ilg et al., 1996). The supracrustal suite is in transposed depositional contact with underlying basement of the 1840 ± 1 Ma Elves Chasm Gneiss, an orthogneiss that ranges from hornblende biotite tonalite to granodiorite (Hawkins et al., 1996). The Elves Chasm Gneiss is the oldest presently known rock in southwestern North America and is ~90 Ma older than all other lithologies in the Grand Canyon region.

The plutonic rocks of the Granite Gorges are calc-alkaline plutons, 1741–1713 Ma in age (Hawkins et al., 1996), interpreted as subduction-related arc plutons; they are primarily granodiorite and commonly have gabbro-diorite enclaves that record varying degrees of magma mixing (Babcock et al., 1979; Ilg et al., 1996; Karlstrom et al., 2003). Some contacts with the country rock are intrusive with crosscutting fabric relations, but many are tectonic contacts (Table 1). The largest plutons are 10-km-scale, large F_2-folded sheet-like bodies, while others are kilometer-wide subvertical tabular bodies that suggest tectonic slices (Fig. 3). Ultramafic cumulates occur as lenses within turbidites and are interpreted as dismembered roots of arc magma chambers (Seaman et al., 1997). The 1.70–1.66 Ga granite-pegmatite dike swarms are interpreted to be syncollisional granites derived from partial melting of a tectonically thickened crust (Ilg et al., 1996; Hawkins et al., 1996).

The tectonic history of the Upper Granite Gorge involves multistage deformation and metamorphism culminating in the 1.72–1.68 Ga Yavapai orogeny (Ilg et al., 1996; Dumond et al., 2007). Structural, geochronologic, and metamorphic studies suggest that the two main stages of deformation overlap locally, and peak metamorphism occurred synchronously with the transition between D_1 and D_2 (Ilg et al., 1996). D_1 involved early thrusting and isoclinal folding, preserved in domains of NW-striking S_1 fabric developed between 1730 and 1698 Ma (Ilg et al., 1996). D_2 involved kilometer-scale upright, isoclinal to open F_2 folds and development of a penetrative NE-striking subvertical S_2 foliation from 1713 to 1685 Ma (Ilg et al., 1996; Dumond et al., 2007). This subvertical foliation is the dominant fabric throughout the transect. The block-bounding high-strain zones (Fig. 2) are in D_2 orientations, but they probably accommodated multiple slip events, including earlier D_1 movements and later brittle displacement that affected the Grand Canyon Supergroup (Huntoon et al., 1980; Elston, 1989). Metamorphic studies indicate variable peak temperatures of 520–770 °C, with the high-strain zones serving as 100–200 °C thermal discontinuities between tectonic blocks at near isobaric ~0.7 GPa pressure (~25 km depth; Ilg et al., 1996; Dumond et al., 2007). Dumond et al. (2007) proposed that changes in peak metamorphic temperature across shear zones were the result of magma-enhanced metamorphic field gradients and that the entire transect decompressed from ~0.7 to ~0.3–0.4 GPa (~12 km depths) mainly during the end of D_2 by 1680 Ma, or perhaps as late as 1.4 Ga.

Shear zones are primarily D_2 shortening high-strain zones; however, some have been proposed to have earlier histories, like the Crystal shear zone. It is an ~1-km-wide, NE-striking zone of strong foliation with stretching lineations plunging steeply to the west (Ilg et al., 1996). Based on macroscopic fold asymmetries, and an ~0.1 GPa higher pressure to the west (Ilg et al., 1996; Dumond et al., 2007), the shear zone is interpreted as a dip-slip fault that accommodated west-side-up slip. The presence of possible mélange-like rocks, a step to more radiogenic common Pb isotopic composition west of the shear zone, and the presence of xenocrystic >2.0 Ga zircons to the west of the shear zone suggest that the Crystal shear zone represents an early (D_1) structure that was reactivated and transposed during D_2 deformation (Ilg et al., 1996; Hawkins et al., 1996). However, as mentioned already, the uniform detrital zircon population of the Vishnu Schist across this boundary suggests that any juxtaposition of crustal blocks across this boundary must have occurred before or during Vishnu Schist deposition at 1750 Ma (Shufeldt et al., 2010).

METHODS

Samples for this study were collected over the course of several field seasons from 2005 to 2014, and U-Pb and Hf isotopic analyses were conducted at two different laboratories. Plutonic samples from western Grand Canyon were taken during two field seasons in 2005–2006 and analyzed at the Geochemical Evolution and Metallogeny of Continents (GEMOC) Key Centre at Macquarrie University in Sydney, Australia. Samples of Vishnu Schist from across the entire Grand Canyon transect were taken during field seasons in 2005–2006 and 2008, and detrital zircon U-Pb analyses were conducted at the Arizona LaserChron Center (ALC) at the University of Arizona in Tucson, Arizona. Subsequent Hf isotopic analysis of the Vishnu Schist was carried out on these samples at the ALC in 2010 and 2012–2014. Plutonic samples from the eastern Grand Canyon were collected and analyzed at the ALC during 2012–2014. Analytical methods at both laboratories are detailed in GSA Data Repository[1] (see also Belousova et al., 2001; Griffin et al., 2000, 2002, 2004; Jackson et al., 2004; Gehrels et al., 2006, 2008; Cecil et al., 2011; Gehrels and Pecha, 2014).

As detailed in the GSA Data Repository (see footnote 1), both laboratories employ similar sample preparation and analytical methods and report similar precision and accuracy in both U-Pb and Hf isotopic analyses. Both laboratories perform standard heavy mineral separation techniques and mount unknowns together with zircon standards. Prior to analysis, backscattered electron (BSE) or cathodoluminescence (CL) images of all unknown grains were obtained to guide spot selection and identify potential xenocrystic cores. All ε_{Hf} values were calculated using the bulk silicate earth composition of Bouvier et al. (2008), and we compare the results to the depleted mantle composition of Vervoort and Blichert-Toft (1999).

U-Pb AND Hf ICP-MS RESULTS FROM GRAND CANYON

Table 1 provides a synthesis of new and published U-Pb geochronologic and Hf isotopic analyses from the basement rocks of the Grand Canyon organized from east to west in the transect and keyed to Figure 3. Supporting data are presented in more detail in the GSA Data Repository material (see footnote 1).

Interlaboratory Comparison

Samples of the Tuna Creek pluton and the Elves Chasm gneiss were independently analyzed at both laboratories. Before discussion and interpretation of the U-Pb-Hf isotopic data discussed herein, we compare the results from these very different samples. The Tuna Creek pluton and the Elves Chasm gneiss provide an excellent means of interlaboratory comparison; the Tuna Creek pluton contains a complex zircon population with varied U-Pb ages and Hf isotopic compositions and has never been precisely dated. In contrast, the age of the Elves Chasm gneiss is precisely known (Hawkins et al., 1996), and results from both laboratories show that it is juvenile at 1840 Ma. Therefore, as discussed in more detail later herein, similar U-Pb-Hf characteristics reported from each laboratory show consistent results, and the data can be presented and interpreted together.

Elves Chasm Gneiss

Sample K05–113 was analyzed at the GEMOC Key Centre, and sample K12–115L was analyzed at the ALC. The results of each sample analysis are compared in Figure 4. Twenty grains separated from sample K05–113 (GEMOC) yield a weighted mean age of 1841 ± 5 Ma (mean square of weighted deviates [MSWD] = 0.7). Likewise, 12 ages from sample K12–115L (ALC) yielded a weighted mean age of 1855 ± 18 Ma (MSWD = 0.2). The results from both laboratories are in good agreement with the 1840 ± 1 Ma thermal ionization mass spectrometry (TIMS) age of the Elves Chasm gneiss (Hawkins et al., 1996).

Both samples yielded juvenile $\varepsilon_{Hf(t)}$ values for the Elves Chasm gneiss. Using the bulk silicate earth composition of Bouvier et al. (2008), and the depleted mantle composition of Vervoort and Blichert-Toft (1999), the $\varepsilon_{Hf(t)}$ value of the depleted mantle at 1840 Ma is +9.8. The $\varepsilon_{Hf(t)}$ values from sample K05–113 range from +12.5 to +8.7, with an average of +10.5. Similarly, sample K12–115L yielded $\varepsilon_{Hf(t)}$ values from +11.3 to +6.1, with an average of +8.6. The $\varepsilon_{Hf(t)}$ values from the GEMOC sample (K05–113) were consistently higher than those from the ALC sample (K12–115L), but there was substantial overlap between the two data sets, and all zircons yielded $\varepsilon_{Hf(t)}$ values that are within analytical uncertainty of the depleted mantle array.

Tuna Creek Pluton

Two samples of the Tuna Creek pluton were collected; K05–100.5 was analyzed at the GEMOC Key Centre, and 13H-99R was analyzed at the ALC (Fig. 5). Both samples show excellent agreement in terms of zircon ages; with a 1740 Ma age peak, and a xenocrystic population of 2480–2485 Ma. The presence of inheritance in the Tuna Creek pluton has been documented previously (Hawkins et al., 1996), but the age constraints were limited to crystallization at 1750–1710 Ma with older than 2.0 Ga inheritance. These results corroborate prior findings and provide more complete geochronologic constraints on the age of inherited grains.

There is more disparity between $\varepsilon_{Hf(t)}$ values in the Tuna Creek pluton than the Elves Chasm gneiss. GEMOC $\varepsilon_{Hf(t)}$ values for six ca. 1.74 Ga zircons from the Tuna Creek pluton plot in a tight cluster at ~+2.8. Two additional grains yielded lower values; one zircon yielded an $\varepsilon_{Hf(t)}$ value of −11.3 at 1853 Ma. This grain overlaps at 2σ with the age of the Elves Chasm gneiss, but it has a substantially lower $\varepsilon_{Hf(t)}$ value. The 2.48 Ga xenocrystic population in the GEMOC sample also plots in a tight cluster, with an average $\varepsilon_{Hf(t)}$ value of −1.2 for six grains. Conversely,

[1]GSA Data Repository item 2015158, Table DR1, new Vishnu Schist and Rama Schist U-Pb geochronologic analyses; Table DR2, Vishnu Schist and Rama Schist Hf isotopic analyses; Table DR3, plutonic U-Pb geochronologic analyses conducted at the Arizona LaserChron Center (ALC); Table DR4, plutonic Hf isotopic analyses conducted at the ALC; Table DR5, plutonic U-Pb analyses conducted at the Geochemical Evolution and Metallogeny of Continents (GEMOC) Key Centre, Macquarie University; Table DR6, plutonic Hf isotopic analyses conducted at the GEMOC Key Centre; descriptions of individual plutonic sample zircon ages, morphology, and internal textures, concordia plots and weighted mean ages for each sample, epsilon Hf plots for each sample, and cathodoluminescence images of each grain, is available at http://www.geosociety.org/pubs/ft2015.htm or by request to editing@geosociety.org.

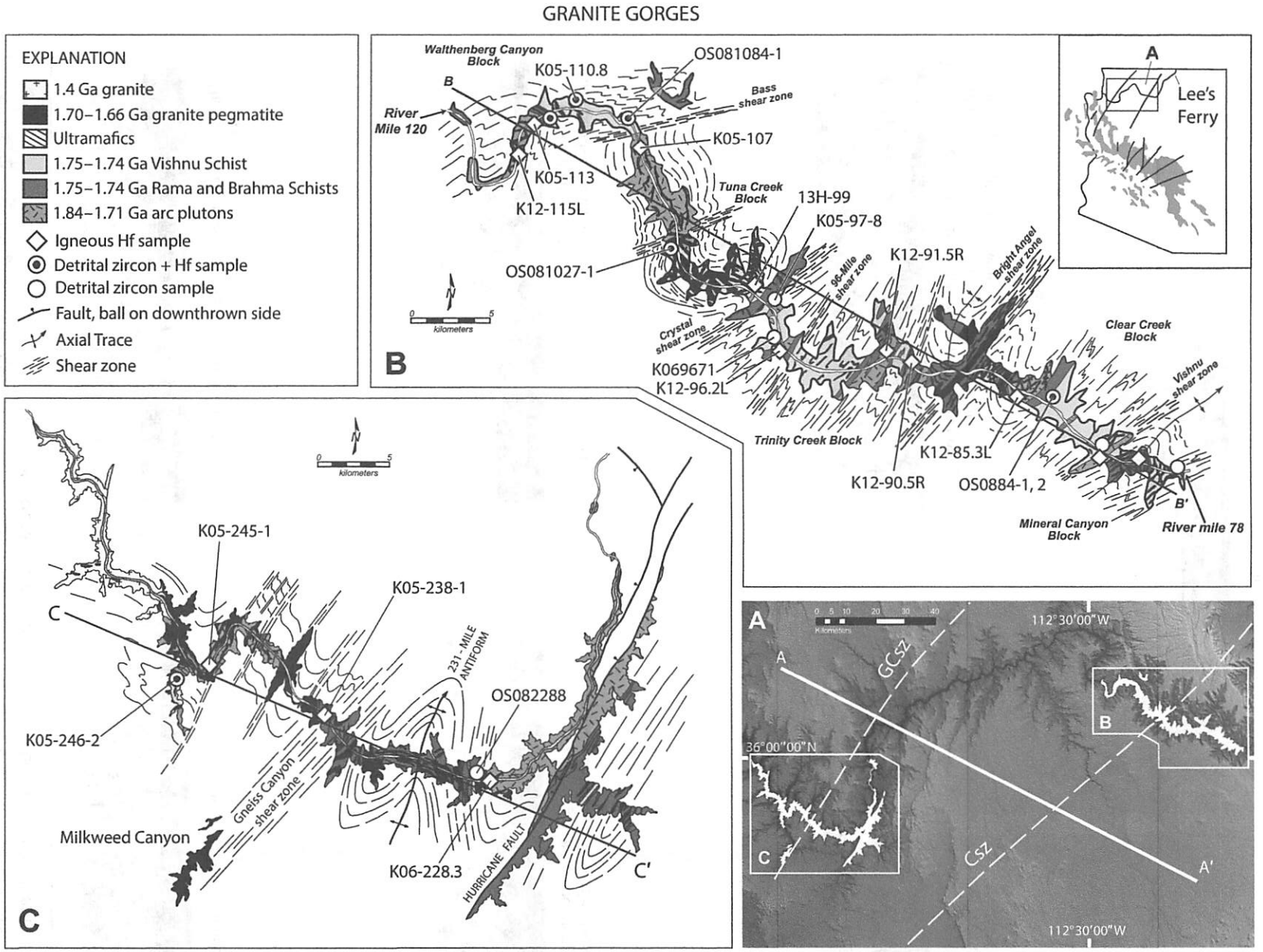

Figure 2. (A) Digital elevation model of the Grand Canyon region. Paleoproterozoic outcrops are shown in white. Csz—Crystal shear zone, GCsz—Gneiss Canyon shear zone. Line of section A to A′ is keyed to Figure 14. (B) Geologic map of the Upper Granite Gorge after Ilg et al. (1996). Line of section B to B′ is keyed to Figure 3A. Inset shows the Colorado River, with outcrops of Proterozoic rocks in the Arizona transition zone shown in gray. Sample locations are projected orthogonally from their location along the river corridor to the line of section. (C) Geologic map of the Lower Granite Gorge after Karlstrom et al. (2003). Line of section C to C′ is keyed to Figure 3B. Sample locations are projected orthogonally from their location along the river corridor to the line of section.

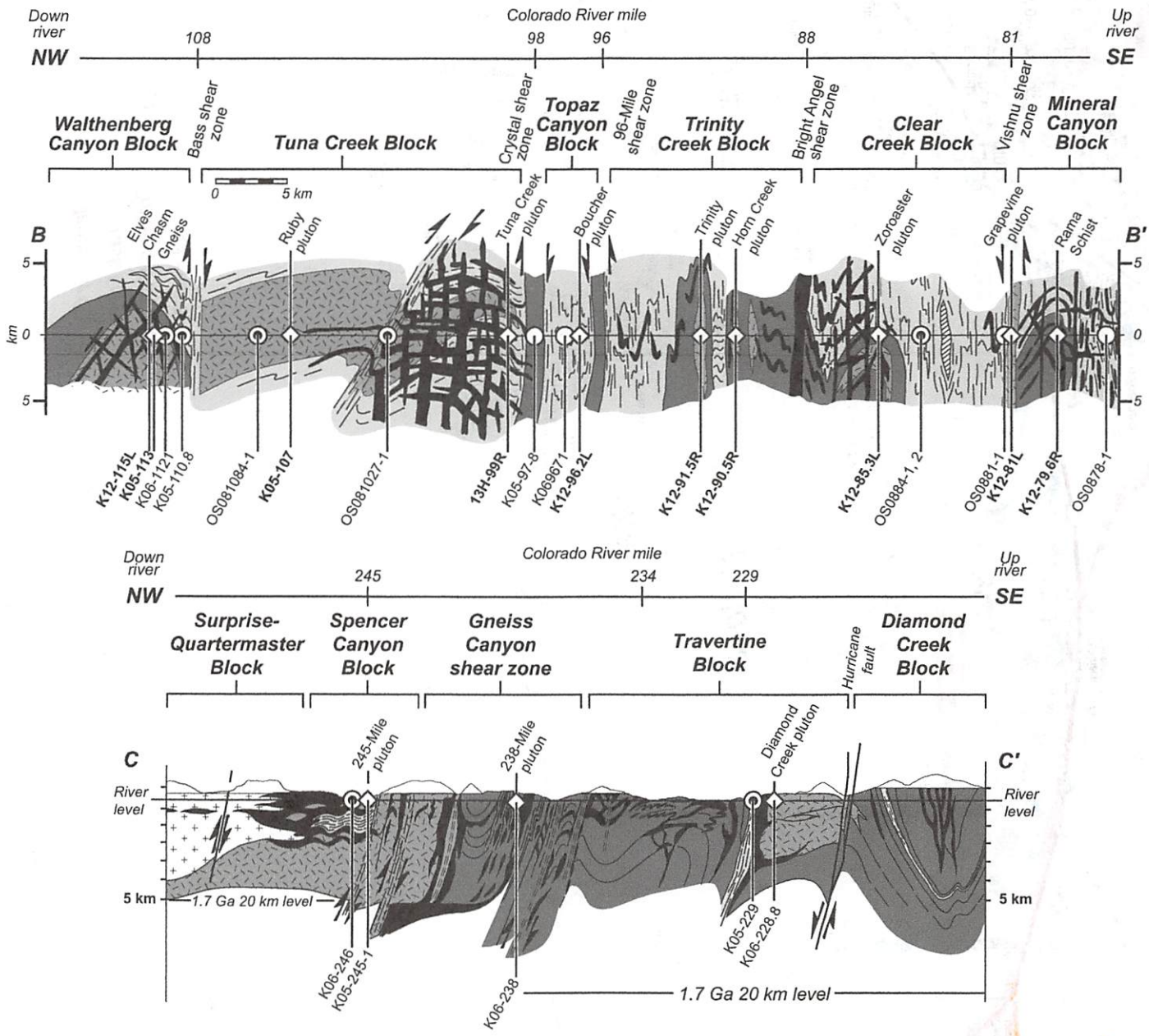

Figure 3. Geologic cross sections of the Upper and Lower Granite Gorges modified after Dumond et al. (2007) and Karlstrom et al. (2003), respectively. Sample locations are projected orthogonally from the river corridor to the line of section. The block-type architecture and block-bounding high-strain zones are shown along with river mile downstream of Lee's Ferry.

the ALC $\varepsilon_{Hf(t)}$ values for the 1740 Ma population show more of a vertical spread, with $\varepsilon_{Hf(t)}$ values of seven grains ranging from +2.8 to +12.7 and averaging +7.1. Three additional grains that overlap with the age of the Elves Chasm gneiss were identified in sample 13H-99R; two yielded juvenile $\varepsilon_{Hf(t)}$ values, and one yielded an intermediate value of –3.7 at 1851 Ma. Finally, the ca. 2.48 Ga population of zircons yielded $\varepsilon_{Hf(t)}$ values ranging from +0.9 to +3.7 and averaging +2.2.

Comparison Summary

Hf isotopic data from each sample show substantial overlap; however, average values consistently differ by ~2 epsilon units. These differences are within uncertainty of the $\varepsilon_{Hf(t)}$ values. The $\varepsilon_{Hf(t)}$ values for the Elves Chasm gneiss were consistently higher from the GEMOC data; however, the ALC data yielded higher $\varepsilon_{Hf(t)}$ values for the Tuna Creek pluton. As described by Gehrels and Pecha (2014), the uncertainties reported by the ALC are "not of ideal precision," due to analytical procedures that emphasize accuracy at the expense of internal precision. The result of these procedures is that the $\varepsilon_{Hf(t)}$ values reported by the GEMOC Key Centre are more precise. However, standard analyses from the ALC yielded uncertainties of ±0.000035 (May 2013) to ±0.000040 (May 2014) at 1σ, which result in standard uncertainties of 2–3 epsilon units at the 2σ level. The uncertainty in standard analyses is consistent with the ~2 epsilon unit disparity between the ALC and

TABLE 1. GEOCHRONOLOGIC DATA OF IGNEOUS BASEMENT ROCKS IN GRAND CANYON

Sample no.	Lat and long (°N, °W)	Rock name/type	River mile	Weighted mean U-Pb age (Ma)	MSWD	Hf isotopic character	Deformational context	Contact relations	Metamorphic block	Laboratory
K12-79.6R	36.0504 111.969052	Rama Schist	79.6	1751 ± 16 1741 ± 1[1]	0.2	Juvenile	Pre-D_1; from hinge of Sockdolager antiform	Interlayered with Vishnu Schist	Mineral Canyon	ALC
K12-81L	36.054487 111.996103	Grapevine Camp pluton	81	1756 ± 16 1737 ± 1[1]	0.3	Juvenile	Contains S_1; aligned along S_2 Vishnu shear zone; pre-D_1	Crosscuts compositional layering in Vishnu Schist on eastern contact; western contact is the Vishnu shear zone	Mineral Canyon	ALC
K12-85.3L	36.089238 112.0595978	Zoroaster pluton	85.3	1755 ± 14 1740 ± 2[1]	0.6	Juvenile	Contains S_1, folded by F_2; pre- or syn-D_2	Contains screens of Grand Canyon metamorphic suite	Clear Creek	ALC
K12-90.5R	36.102022 112.1372997	Horn Creek pluton	90.5	1719 ± 14 1713 ± 1[1]	0.3	Juvenile	Contains magmatic S_1, solid state S_2; syn-D_1	Intrudes parallel to compositional layering in Vishnu Schist	Trinity Creek	ALC
K12-901.5R	36.106201 112.1537577	Trinity Gneiss	91.5	1755 ± 16 1730 ± 3[1]	0.4	Juvenile	Contains S_1 and S_2; pre-D_1	Contacts between Brahma amphibolites are folded and sheared; intrusive contacts locally preserved	Trinity Creek	ALC
K12-96.2L	36.109483 112.2271762	Boucher pluton	96.2	1730 ± 15 1714 ± 1[2]	0.5	Juvenile with inherited Archean grains	Weakly foliated; pre or syn-D_1	Eastern margin is 96-Mile shear zone; western margin is intrusive into metasupracrustals	Topaz Canyon	ALC
13H-99R	36.144397 112.2551292	Tuna pluton	99	1751 ± 15 < 1750[1]	1.1	Mixed juvenile with Archean inheritance	Contains S_1 and S_2; pre- to syn-D_1	Folded sheet-like body intrudes Vishnu Schist	Tuna Creek	ALC
K05-100.5-105	36.14341 112.27587	Tuna pluton	100.5	1737 ± 7 < 1750[1]	0.7	Mixed juvenile with Archean inheritance	Contains S_1 and S_2; pre- to syn-D_1	Folded sheet-like body intrudes Vishnu Schist	Tuna Creek	GEMOC
K05-107	None provided	Ruby pluton	107	1726 ± 15 1716.6 ± 0.5[1]	0.1	Juvenile	Contains S_1 as magmatic layering; syn-D_1	Eastern margin is tectonized, but locally preserves intrusive relations to supracrustal rocks; western margin is cut by the Bass shear zone	Tuna Creek	GEMOC
K06-113	36.2271 112.422779	Elves Chasm Gneiss	113	1842 ± 5 1840 ± 1[1]	0.9	Juvenile	Contains S_1 and S_2; pre-D_1 basement to Vishnu Schist	Transposed depositional contact between Brahma Schist and Elves Chasm Gneiss	Walthenberg Canyon	GEMOC
K12-115L	36.203657 112.42610	Elves Chasm Gneiss	115	1850 ± 18 1840 ± 1[1]	1.4	Juvenile	Contains S_1 and S_2; pre-D_1 basement to Vishnu Schist	Transposed depositional contact between Brahma Schist and Elves Chasm Gneiss	Walthenberg Canyon	ALC
K06-228.3	35.75249 113.54806	Diamond Creek pluton	228.3	1738 ± 14 1736 ± 1[3]	0.2	Juvenile with 1.8 Ga inheritance	Contains magmatic S_1 and solid-state S_2 shear zones; syn-D_1	Intrudes Vishnu Schist on western margin; eastern margin covered by Phanerozoic rock	Travertine block	GEMOC
K06-238-1	35.7969 113.54806	Granitic gneiss from Gneiss Canyon shear zone	238	1731 ± 14	0.1	Mixed juvenile with Archean inheritance	Cuts S_1, contains weak to strong and magmatic S_2; syn-D_2	Sheet-like intrusions into mixed paragneisses and orthogneisses	Gneiss Canyon shear zone	GEMOC
K06-245-2	35.82113 113.62846	245-Mile pluton	245	1741 ± 13 1720 ± 5[3]	0.6	Juvenile with Archean inheritance	Contains S_1 and S_2; pre-D_2	Intrudes into Vishnu Schist on western margin; eastern margin is intruded by the younger Separation pluton	Spencer Canyon block	GEMOC

Note: All uncertainties are reported at 2σ. MSWD—mean square of weighted deviates; ALC—Arizona LaserChron Center; GEMOC—Geochemical Evolution and Metallogeny of Continents Key Centre. Sources for previous ages are: 1—Hawkins et al. (1996); 2—Hawkins (1996); 3—Karlstrom et al. (2003). Field relations are from Ilg et al. (1996) and Karlstrom et al. (2003). Pluton descriptions are from Hawkins et al. (1996).

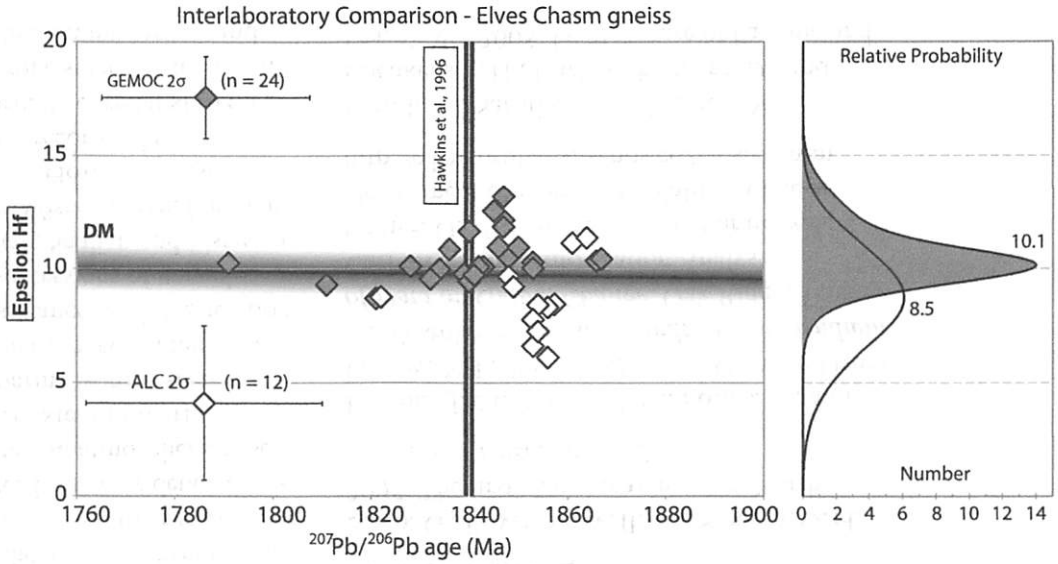

Figure 4. Comparison of results from the Elves Chasm Gneiss as analyzed at the Geochemical Evolution and Metallogeny of Continents (GEMOC) Key Centre, and the Arizona LaserChron Center (ALC). Symbols with error bars represent the average 2σ uncertainties for U-Pb and Lu-Hf isotopic analyses from each data set. DM—depleted mantle.

GEMOC Key Centre and suggests that all measurements are accurate to within 2–3 epsilon units. While sample pairs K05–113, K12–115L, and K05–100.5, 13H-99R were obtained from the same plutons, analyses were not conducted on the same zircons. It is possible that one or both plutons may not be isotopically homogeneous, and that the observed variation in $\varepsilon_{Hf(t)}$ values reflects real isotopic variation within the plutons. In conclusion, we feel that the results from each laboratory are consistent, and the entire data set can be compared within reasonable uncertainty.

Results from Supracrustal Rocks

Vishnu Schist

We obtained 380 new U-Pb ages from Vishnu Schist for this study. Analyses were conducted on the same grain mounts prepared by Shufeldt et al. (2010) with the intention of obtaining paired U-Pb and Hf isotopic data. We selected samples that were distributed across the entire length of the Grand Canyon transect (RM 84–246) to obtain data that are representative of the entire population. The results of each analysis are presented in Table DR1 (see footnote 1).

Our new data are compiled with the entire data set of Shufeldt et al. (2010) and presented in order from east to west (RM downstream of Lee's Ferry) in Figure 6. New samples show the same bimodal Paleoproterozoic and earliest Paleoproterozoic populations with peaks at 1780 Ma and 2480 Ma as identified by Shufeldt et al. (2010), and they confirm the observation that, whereas individual samples vary, there is no systematic difference in the relative proportions of the 2.5 and 1.8 Ga age populations from east to west across the Crystal shear zone. Shufeldt et al. (2010) reported that only 13% of all grains overlapped at 2σ with the 1750–1740 Ma depositional age of the Vishnu Schist (Hawkins et al., 1996); new data show more grains of this age (Fig. 6), such that the new composite Vishnu distribution has 18% 1740–1750 Ma first-cycle grains. Also, 14% of all ages overlap at 2σ with the 1840 ± 1 Ma Elves Chasm gneiss, and 28% are >2500 Ma in age.

We obtained Hf isotopic information for 187 zircons from six spatially distributed samples of Vishnu Schist (Fig. 7). The results of each individual analysis are presented in Table DR2 (see footnote 1). As for the U-Pb ages, there is variation in which mode dominates a given spectrum, but there is no systematic variation in Hf composition with river mile (Fig. 7). For example, sample K0598.6–104 did yield Archean U-Pb ages (Fig. 6), but each of these grains was either too small to withstand the larger spot size and deeper pit depth of Hf analysis, or the Hf analyses did not pass the data reduction process. The apparent difference in detrital zircon age spectra in this case is probably the result of a reduced sample size for this sample (n = 32 for U-Pb, and n = 16 for Hf). However, we do not feel that the Hf isotopic data for the Archean population is underrepresented in the entire data set.

Detrital zircons from the Vishnu Schist yield a broad range of $\varepsilon_{Hf(t)}$ values from +10.0 to –19.4. Following Bahlburg et al. (2011), $\varepsilon_{Hf(t)}$ values within five epsilon units of the depleted mantle array are considered juvenile. Surprisingly, only 30 grains (16%) of the entire Vishnu Schist data set yielded juvenile values. However, due to the time-integrated nature of Hf isotopic information, these terms refer to the zircons themselves compared to depleted mantle rather than compared to depositional age. Thus, for our purposes, only zircons that yield crystallization ages of 1750–1740 Ma as well as $\varepsilon_{Hf(t)}$ values that overlap at 2σ with the depleted mantle array, and therefore could have been derived from local arc rocks, are considered juvenile. Of the 187 grains for which we have paired U-Pb-Hf data, 58 grains (31%) fall in this age range, and only 14 of those grains (6%) yield $\varepsilon_{Hf(t)}$ values within five epsilon units of depleted mantle. Therefore, we infer that only 6% of grains could have been derived from juvenile (1.75–1.74 Ga) sources (see following). The rest were derived from older crust.

Shufeldt et al. (2010) proposed that the 1.8 Ga age peak in the Vishnu Schist was derived from the Elves Chasm Gneiss, a hypothesis which is tested with our new Hf isotopic data. Twenty-three grains for which we have paired U-Pb-Hf isotopic data overlap at 2σ with the 1840 ± 1 Ma Elves Chasm Gneiss. However, only 4 yielded $\varepsilon_{Hf(t)}$ values that overlap with the depleted mantle array. Therefore, the Elves Chasm Gneiss was not a significant source of detrital zircons in the Vishnu Schist. Our data show that very little of the detritus that formed the protolith of the Vishnu Schist was derived from local crust. Instead, Vishnu Schist was overwhelmingly derived from older, isotopically evolved crust.

Rama Schist

A sample of the Rama Schist was collected from the same locality sampled by Hawkins et al. (1996). A weighted mean of 12 analyses yielded an age of 1751 ± 16 Ma (MSWD = 0.2), in good agreement with the 1741 ± 1 Ma age of Hawkins et al. (1996).

The 10 grains for which we obtained Hf isotopic data yielded juvenile $\varepsilon_{Hf(t)}$ values that

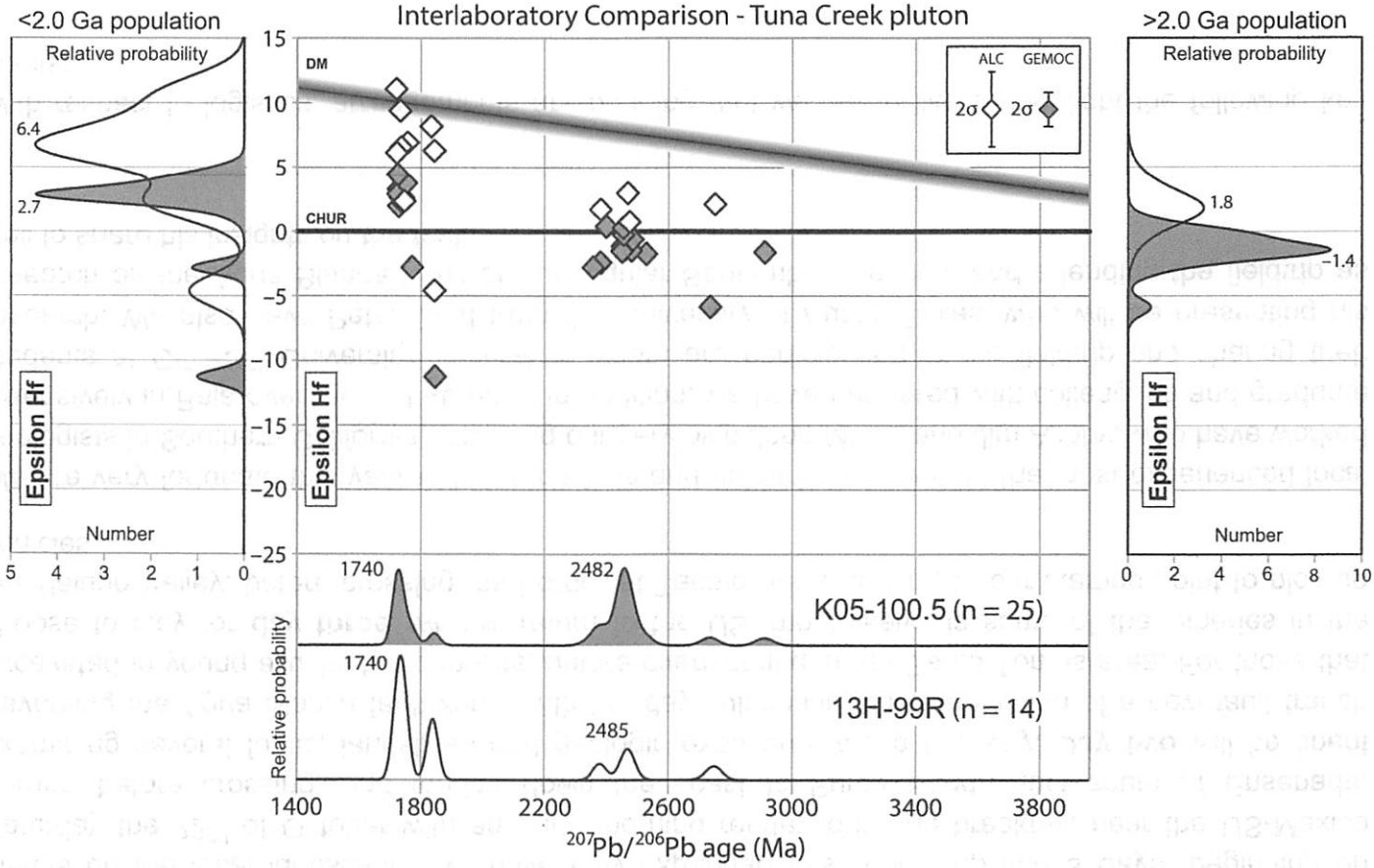

Figure 5. Comparison of Arizona LaserChron Center (ALC) and Geochemical Evolution and Metallogeny of Continents (GEMOC) Key Centre results for the Tuna Creek pluton. Coloring and symbols are as in Figure 4. For ease of visual comparison, age probability plots are normalized such that the area beneath each curve is equal. Age probability plots show excellent agreement between U-Pb ages in primary and inherited grains. DM—depleted mantle; CHUR—chondritic uniform reservoir.

ranged from +5.7 to +11.3 (Fig. 7). All but one grain yielded $\varepsilon_{Hf(t)}$ values that overlap with the depleted mantle array. This is the same range of $\varepsilon_{Hf(t)}$ values shown by plutons in eastern Grand Canyon (see following), which suggests that the interlayered metavolcanics were locally derived juvenile arc products and that they became interlayered with far-traveled sedimentary rocks derived from older crustal sources. Interlayering is now parallel to strong S_2 foliation such that it could have been primary or tectonic, an interpretation that would require additional study.

Results from Granodiorite Plutons

East of Crystal Shear Zone

We obtained 153 U-Pb ages from zircons separated from five plutons east of the Crystal shear zone from RM 81 to 96 (Fig. 8). In total, 84 grains (74%) overlap at 2σ with the 1741–1713 Ma timing of arc magmatism described by Hawkins et al. (1996). Although there are individual outliers, and ICP-MS precision is considerably less than the previous isotope dilution (ID) TIMS dates, weighted mean ages for each pluton are in good agreement with previously published ID-TIMS ages (Table 1).

Hf isotopic data for plutonic zircons east of the Crystal shear zone are shown in Figure 8. We obtained paired U-Pb-Hf isotopic data for 97 plutonic zircons. $\varepsilon_{Hf(t)}$ values range from –5.1 to +13.1, however this range is due to two outliers that yielded negative values (see below). 95 of the 97 analyses yielded $\varepsilon_{Hf(t)}$ values that define a smaller range from +5.5 to +13.1. Of the 97 analyses, 86 (87%) of them yielded $\varepsilon_{Hf(t)}$ values that overlap with the depleted mantle array. They form a very tight cluster that indicates these granodiorites were derived almost entirely from a juvenile source. However, the few grains that yielded more-evolved $\varepsilon_{Hf(t)}$ values suggest minor involvement of slightly older juvenile crust, such as the Elves Chasm Gneiss, or a crustal component as old as 2.0 Ga.

Two of the grains that do not overlap with the depleted mantle array are core analyses from the Boucher pluton: K12–96.2L-22C, which yielded an $\varepsilon_{Hf(t)}$ value of –5.1 at 1945 Ma, and K12–96.2L-17C, which yielded an $\varepsilon_{Hf(t)}$ value of –2.9 at 2483 Ma. Grain K12–96.2L-1C yielded a juvenile $\varepsilon_{Hf(t)}$ value of +8.7 at 1839 Ma. The Boucher pluton at RM 96 (K12–96.2L) contained zircons that displayed inherited cores in CL texture. Twenty-five core-rim pairs were analyzed; however, only eight core-rim pair analyses passed the data reduction process. Many apparent core-rim pairs ultimately yielded overlapping ages that contributed to the 1730 ± 15 Ma weighted mean age. Only one core-rim pair yielded nonoverlapping ages. Grain K12–96.2L-3 yielded a core age of 2598 ± 22 Ma and a rim age of 1727 ± 37 Ma (Fig. 8). In addition, grain K12–96.2L-1 yielded core and rim ages of 1839 ± 19 and 1761 ± 101 Ma, respectively. The large uncertainty associated with the rim analysis causes these grains to overlap at 2σ. We infer that the rims are the same age as the 1730 Ma crystallization age of this pluton. Similarly, despite the lack of reliable rim age data, two additional core

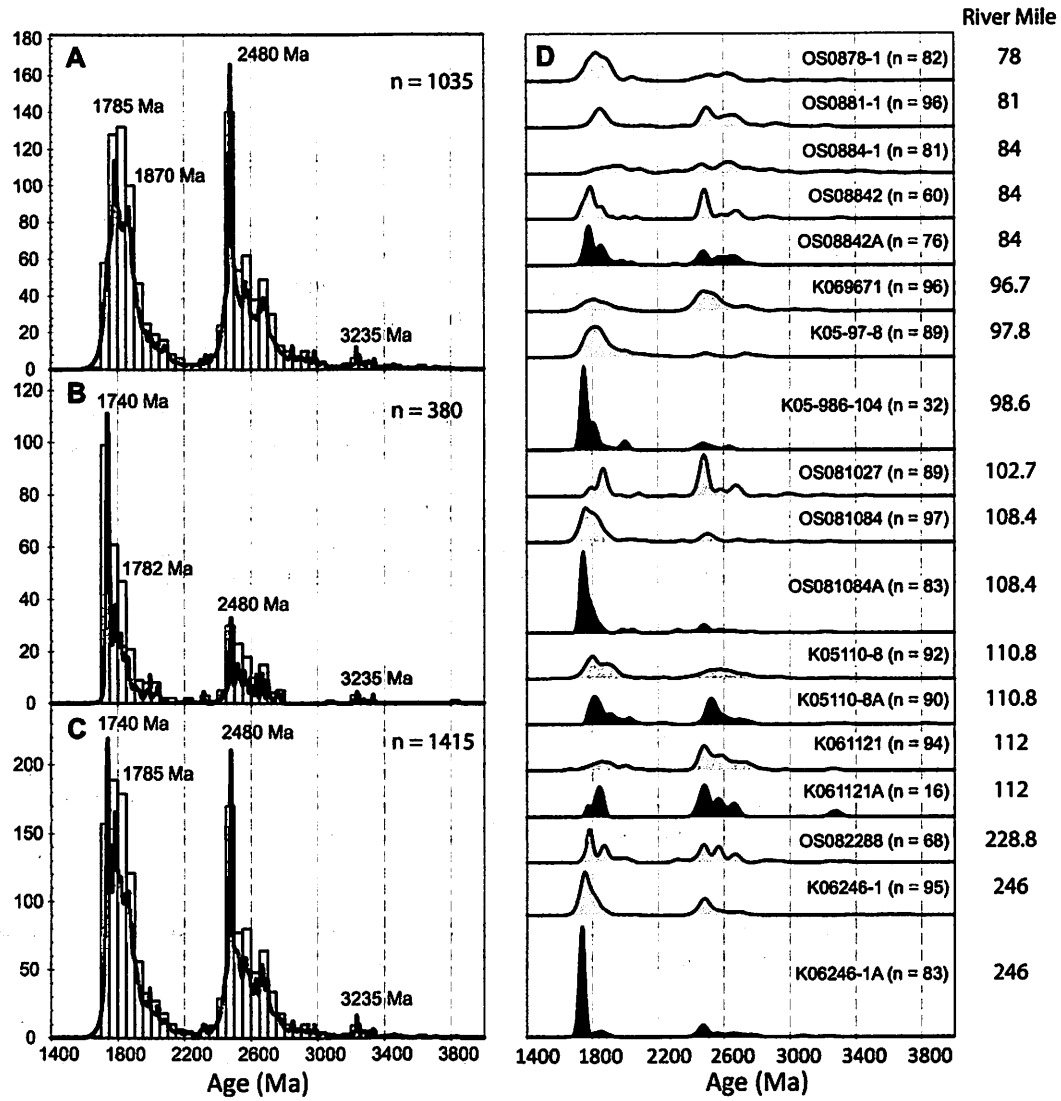

Figure 6. Comparison and synthesis of new and previous Vishnu Schist detrital zircon U-Pb age data. (A) Composite age probability plot taken from Shufeldt et al. (2010). (B) New detrital zircon ages obtained for this study. (C) New composite age probability plot with all current Vishnu Schist detrital zircon ages. (D) Age probability plots of Vishnu Schist detrital zircon samples arranged by river mile (OS0878–1 = Owen Shufeldt [2008], river mile 78), normalized as in Figure 5. Results from Shufeldt et al. (2010) are filled light gray; new results obtained in this study are filled black. See also Table DR1 for detrital zircon age data (see text footnote 1).

analyses yielded ages substantially older than the 1730 Ma population. Grain K12–96.2L-22C yielded an age of 1945 ± 22 Ma, and grain K12–96.2L-17C yielded an age of 2483 ± 24 Ma. The latter age corresponds quite closely to the 2481 Ma age peak defined in the compiled data of the Vishnu Schist (Shufeldt et al., 2010).

West of Crystal Shear Zone

Granodioritic plutons west of the Crystal shear zone are different than those to the east. We obtained 134 paired U-Pb-Hf isotopic analyses from zircons separated from six plutons west of Crystal shear zone from RM 99 to 245 (Fig. 9). Excluding the 36 zircons from the Elves Chasm Gneiss, a majority of 64 grains (65%) overlap at 2σ with the 1741–1713 Ma timing of arc-magmatism in the Upper Granite Gorge. However, the remainder of grains yielded a semicontinuous spectrum of ages ranging from 1741 to 1867 Ma, and a substantially older inherited population ranging from 2275 to 2936 Ma. Thirteen grains (10%) yielded ages that overlap at 2σ with the 2480 Ma age peak in the compiled data for the Vishnu Schist, and eight grains overlap at 2σ with the age of the Elves Chasm gneiss.

Of the 64 grains that overlap with the 1.74–1.71 Ga magmatism, 25 grains (39%) yielded juvenile $\varepsilon_{Hf(t)}$ values; the remaining 39 grains yielded a spread of more-evolved Hf isotopic compositions, with $\varepsilon_{Hf(t)}$ values as low as –2.8 (Fig. 9B). Furthermore, the eight grains that overlapped in age with the Elves Chasm gneiss yielded varied $\varepsilon_{Hf(t)}$ values ranging from +10.3 to –11.3, with four of them juvenile at 1.84 Ga.

The Elves Chasm gneiss yielded exclusively juvenile $\varepsilon_{Hf(t)}$ values. Attempts were made to date apparently distinct core and rim age domains in zircons, but all attempts yielded ages of ca. 1.84 Ga. Along with the Elves Chasm Gneiss, the Ruby pluton and Diamond Creek pluton yielded only juvenile grains, with the exception of one zircon from the Diamond Creek pluton that yielded a juvenile Elves Chasm–aged grain.

The 2275–2936 Ma population of inherited zircons is derived from the Tuna Creek, 238-Mile, and 245-Mile plutons. These xenocrystic grains are generally more evolved than most of the primary Paleoproterozoic grains (Fig. 9).

DISCUSSION

Comparison of Igneous and Metasedimentary Zircons

Our approach of applying paired U-Pb dating and Hf isotopic analysis to both the oldest metasedimentary rocks and the oldest plutons in the orogen provides insight into the earliest evolution of the Mojave and Yavapai Provinces.

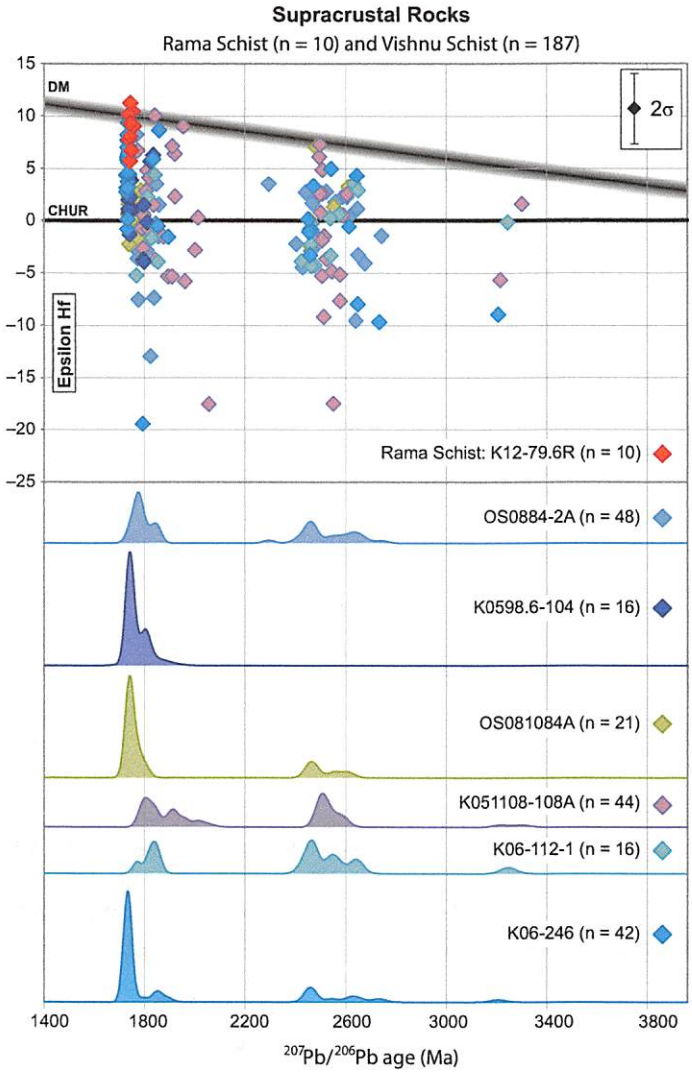

Figure 7. Paired U-Pb-Hf isotopic data for all supracrustal lithologies in Grand Canyon. Each diamond represents a zircon with paired U-Pb and Lu-Hf isotopic data. DM—depleted mantle of Vervoort and Blichert-Toft (1999); CHUR—chondritic uniform reservoir of Bouvier et al. (2008). Sample K12–79.6R is of the Rama Schist (shown in red); all other data are Vishnu Schist. Below are normalized detrital zircon age probability plots of grains for which we have obtained Lu-Hf isotopic data.

These two data sets provide initially contradictory information: Metasedimentary rocks are the same across the proposed Crystal shear zone, whereas plutons are markedly different. The following discussion addresses this apparent conundrum.

Detrital zircons from the Vishnu Schist show a broad range of juvenile and evolved Hf isotopic compositions but are uniform across the entire Grand Canyon transect. The vertical spread of data in epsilon space suggests that the Vishnu Schist was derived from crust that experienced substantial mixing of older crustal material with juvenile magmas, including: ca. 3.3–3.2 Ga crust, ca. 2.8–2.4 Ga crust, and 2.0–1.7 Ga crust, all characterized by mixing of juvenile material with older crust (Fig. 10). Few zircons of any age are juvenile ($\varepsilon_{Hf(t)}$ values that overlap at 2σ with the depleted mantle array) at the time of their crystallization (16%), and most Late Archean grains are dominated by ε_{Hf} values that suggest the involvement of ca. 3.0 Ga crust. The Paleoproterozoic population of zircons implies the involvement of 2.0–2.2 Ga crust, but the lack of crust of that age in our data set, and its relative rarity globally (Voice et al., 2011), might suggest instead that the abundance of Paleoproterozoic grains with $\varepsilon_{Hf(t)}$ values between +5.0 and 0.0 is the result of mixing between juvenile ca. 1.8 and ca. 2.5 Ga crust.

Conversely, interlayered volcanic deposits of the Rama Schist in easternmost Grand Canyon are juvenile at 1.74 Ga. The similarity between plutonic and volcanic $\varepsilon_{Hf(t)}$ values suggests that the Rama Schist in the eastern part of the transect is locally derived from similarly aged, but slightly older, arc magmatism with a predominantly juvenile source.

The age and Hf isotopic composition of plutonic zircons, summarized in Figure 11, are in stark contrast to the detrital grains of the Vishnu Schist. Plutons east of Crystal shear zone are uniformly juvenile at 1.74–1.71 Ga. Few detrital zircons of this age and Hf isotopic composition are found in the Vishnu Schist, suggesting a dearth of local juvenile Yavapai Province–derived crust contributing to the Vishnu basin. However, the xenocrystic grains and Paleoproterozoic grains with more-evolved Hf isotopic compositions found in plutons west of the Crystal shear zone are more similar to Vishnu detritus, which suggests that these plutons interacted with crust similar to crust that provided detritus to the Vishnu basin. Moreover, this may suggest that the Vishnu Schist was derived from the west (present coordinates).

Two important first-order observations are as follows. (1) Granodioritic arc plutons include both juvenile and inherited zircons. (2) There is a dramatic change in igneous zircon ages and Hf composition across the Crystal shear zone: Plutons east of Crystal shear zone yield almost exclusively juvenile $\varepsilon_{Hf(t)}$ values and lack inherited grains. The only exceptions are the two inherited cores found in the Boucher pluton (sample K12–96.2L) at RM 96, which is the westernmost pluton still east of the Crystal shear zone at RM 97 (see following). Conversely, west of the Crystal shear zone, some plutons yield abundant xenocrystic zircons, inherited cores, and more-evolved $\varepsilon_{Hf(t)}$ values, while other plutons are predominantly juvenile. Juvenile plutons include the 1.84 Ga Elves Chasm gneiss (K06–113, and K12–115L), and 1.74–1.71 Ga Grapevine Camp (K12–81L), Zoroaster (K12–85.3L), Horn (K12–90.5R), Trinity (K12–91.5R), Ruby (K06–107), and Diamond Creek (K06–228) plutons. Plutons with inherited signatures include the 1.74–1.71 Ga Boucher (K12–96.2L), Tuna Creek (K06–100.5, and 13H-99R), 238-Mile (K05–238), and 245-Mile (K06–245) plutons.

These data describe a uniform metasedimentary basin that received detritus primarily from isotopically evolved 1.8 and 2.5 Ga crust, which was intruded by a suite of plutonic rocks

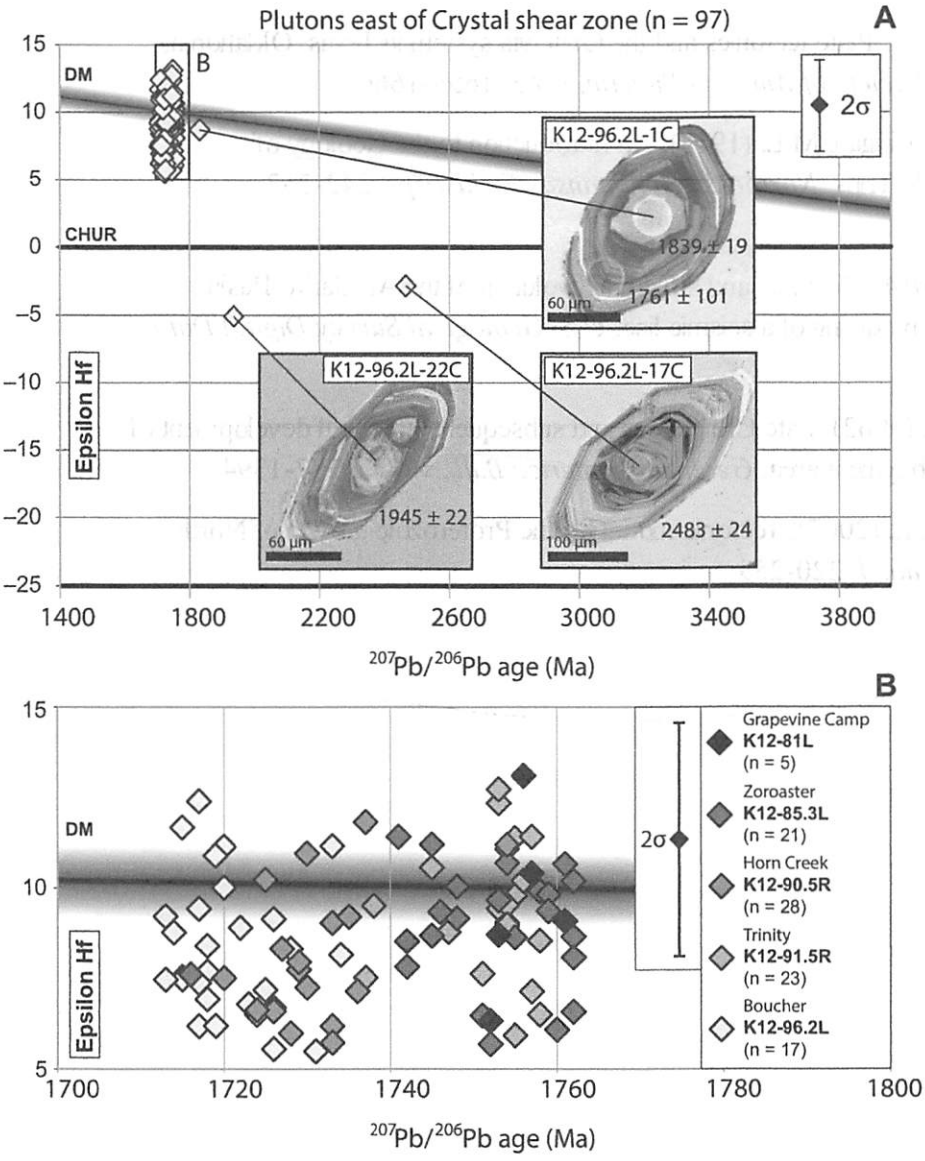

Figure 8. Paired U-Pb-Hf results for zircons separated from plutons east of the Crystal shear zone. Shown above are all results from igneous zircons east of Crystal shear zone. Insets show inverted and gray scaled cathodoluminescent (CL) images of zircons with inherited cores. Shown below are the results for each pluton; note change in *x*-axis scale. Average 2σ uncertainty of all epsilon Hf values is shown in the top right. DM—depleted mantle; CHUR—chondritic uniform reservoir.

with essentially the same crystallization ages but markedly different zircon populations and Hf isotopic compositions across a structural boundary.

Source of the Vishnu Schist

One insight gained from these data is the disparity between the juvenile isotopic signature of the Elves Chasm Gneiss and the more-evolved character of 1.84 Ga detrital grains. Our new data show that Paleoproterozoic detrital zircons yield primarily more-evolved ε_{Hf} values than igneous Elves Chasm Gneiss grains and preclude the interpretation that the Elves Chasm Gneiss contributed a substantial volume of detrital zircons into the Vishnu basin, as suggested by Shufeldt et al. (2010). The presence of additional Penokean-aged crust in central Colorado has been inferred from inherited zircons found in ca. 1.75 Ga granites and rhyolites (Hill and Bickford, 2001). Subsequent Hf isotopic analysis of many of the same samples discussed by Hill and Bickford (2001) included only one grain older than 1800 Ma (aged 1877 ± 37 Ma), which yielded an $\varepsilon_{Hf(t)}$ value of 1.1 (Bickford et al., 2008). This value is substantially lower than $\varepsilon_{Hf(t)}$ values obtained from the Elves Chasm Gneiss, is more similar to $\varepsilon_{Hf(t)}$ values from the ca. 1.85 Ga population of zircons in the Vishnu Schist, and is similar to the somewhat evolved Nd isotopic character of 1.88–1.84 Ga Penokean plutonic rocks (Barovich et al., 1989). It is possible that Penokean-aged crust further to the northeast was the source of the ca. 1.85 Ga population of detrital zircons in the Vishnu Schist; however, one zircon with similar U-Pb-Hf characteristics is not enough to suggest a central Colorado provenance.

The paucity of juvenile first-cycle 1.75–1.74 Ga detrital zircons also precludes the interpretation that local juvenile Yavapai-type plutons contributed substantial detritus to the Vishnu Schist. With the exception of the Elves Chasm Gneiss, plutons exposed in the Grand Canyon intrude the Vishnu Schist and could not have contributed detritus to the Vishnu protolith; however, our data suggest that the Vishnu Schist did not have as its source older juvenile arc terranes such as the 1.78 Ga Green Mountain arc (Jones et al., 2011). In the Gunnison-Salida area, the 1751 Ma Powderhorn Granite yields zircons with evolved $\varepsilon_{Hf(t)}$ values ranging from +2 to +6 (Bickford et al., 2008). Here, 35% of 1.74–1.78 Ga Vishnu grains yielded similar $\varepsilon_{Hf(t)}$ values. In addition, the 1772–1754 Ma Twilight Gneiss of the Needle Mountains is similarly juvenile, and it is old enough to have contributed to the Vishnu Schist (Gonzales and Van Schmus, 2007). Therefore, a modest amount of more locally derived detritus could have been derived from a source area in Colorado; however, it is unlikely that ca. 1.85 Ga crust in Colorado provided the dominant source of Paleoproterozoic detritus to the Vishnu Schist, and even more unlikely that Penokean crust did so.

The inherited Archean-age population and Paleoproterozoic grains with lower ε_{Hf} values suggest that plutons west of the Crystal shear zone might have interacted with the same type of crust that provided detritus to the Vishnu basin. Crust that was the source of the Vishnu Schist might therefore lie to the west (present coordinates). It is likely that the Paleoproterozoic, and possibly Archean, detrital zircon population was derived from the proximal Mojave Province, similar to the model favored by Shufeldt et al. (2010) for the Archean component of the Vishnu Schist. At present, no Elves Chasm Gneiss or older-aged crust has been identified in the Mojave Province, but abundant 1.75–

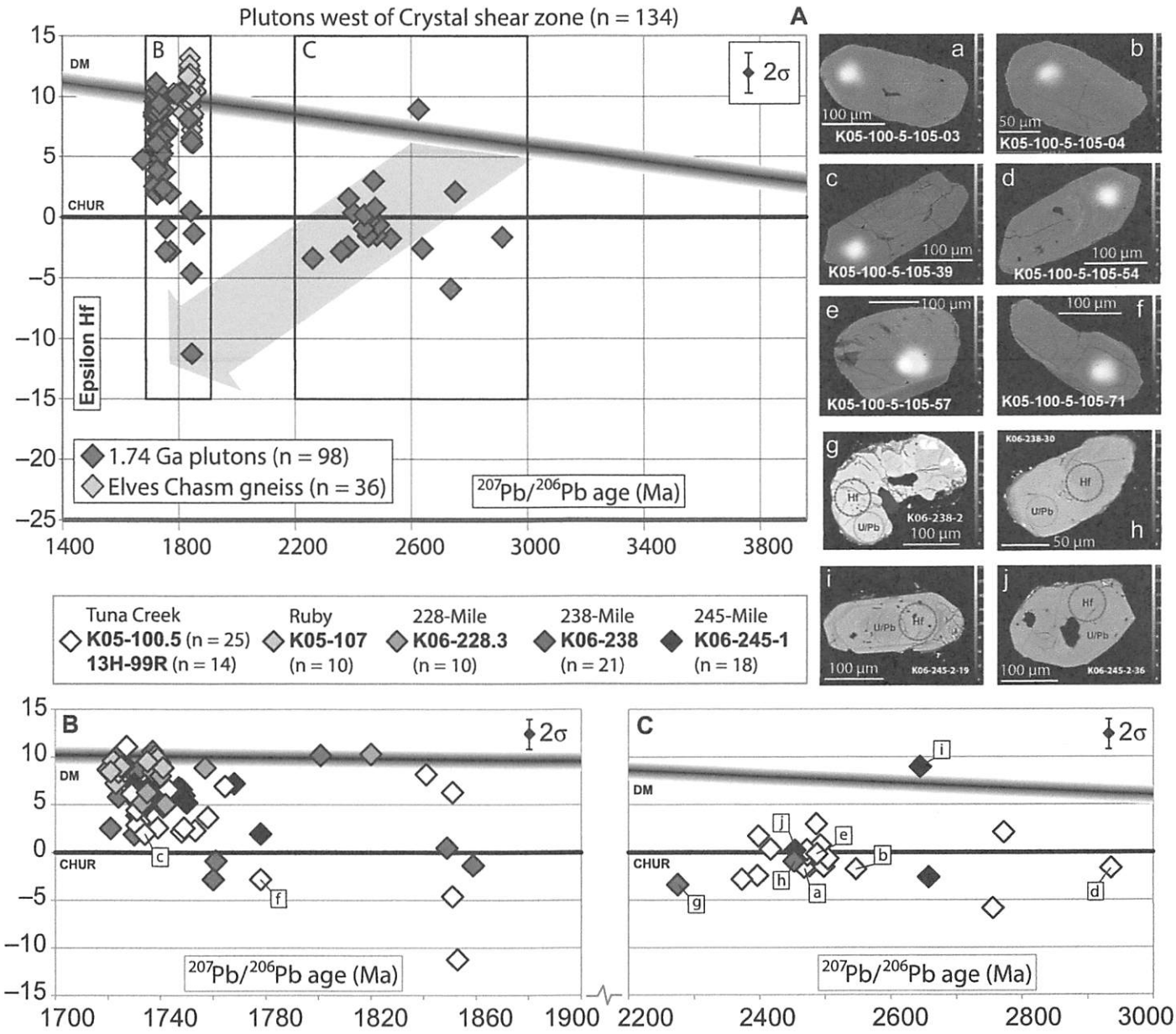

Figure 9. Paired U-Pb-Hf results for zircons separated from plutons west of the Crystal shear zone. (A) Composite diagram of all paired igneous U-Pb-Hf data west of Crystal shear zone. Elves Chasm Gneiss is shown in light gray. Average 2σ uncertainty of all epsilon Hf values is shown in top right. Gray arrow shows average crustal evolution of Vervoort and Patchett (1996). Boxes show area of B and C. (B) Circa 1.7 Ga population of zircons shown according to pluton name and sample number. Elves Chasm Gneiss not shown (see Fig. 4). (C) Inherited population of zircons by sample. (Right) Backscattered-electron (BSE) images of inherited grains and Paleoproterozoic grains with low epsilon Hf values are keyed to B and C. DM—depleted mantle; CHUR—chondritic uniform reservoir.

1.78 Ga granitoids with evolved Nd (Bennett and DePaolo, 1987; Ramo and Calzia, 1998) and Hf (Wooden et al., 2012) compositions exist (Fig. 12). In addition, an Archean component has been recognized in the Nd isotopic composition of the Mojave Province in the Death Valley region (Ramo and Calzia, 1998), and detrital zircons of similar ages to the Vishnu Schist have been documented in the Mojave Province (Barth et al., 2000, 2009; Strickland et al., 2012).

The source of the older than 2.4 Ga population of detrital zircons in the Vishnu Schist remains uncertain. Shufeldt et al. (2010) suggested that the Gawler craton of southern Australia has the most similar age spectrum to the Archean population in the Vishnu Schist; however, recent U-Pb ages obtained from orthogneisses in the Farmington Canyon complex are similar to the 2.48 Ga age peak in the Vishnu Schist (Mueller et al., 2011). The Farmington Canyon complex may be a potential Laurentian source for the older Vishnu Schist detritus; however, the dearth of voluminous Wyoming craton–aged detritus in the Vishnu Schist (Shufeldt et al., 2010) still

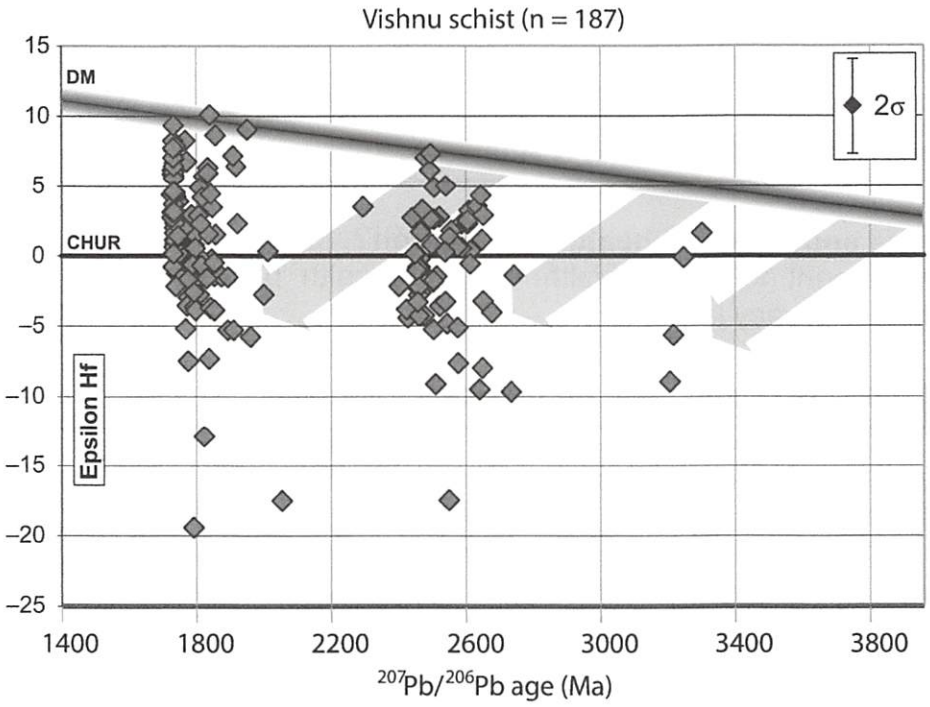

Figure 10. Compiled Vishnu Schist U-Pb-Hf data show that the Vishnu Schist was derived from an Archean craton characterized by extensive crustal reworking at ca. 1.8 Ga, ca. 2.5 Ga, and ca. 3.2 Ga. DM—depleted mantle; CHUR—chondritic uniform reservoir.

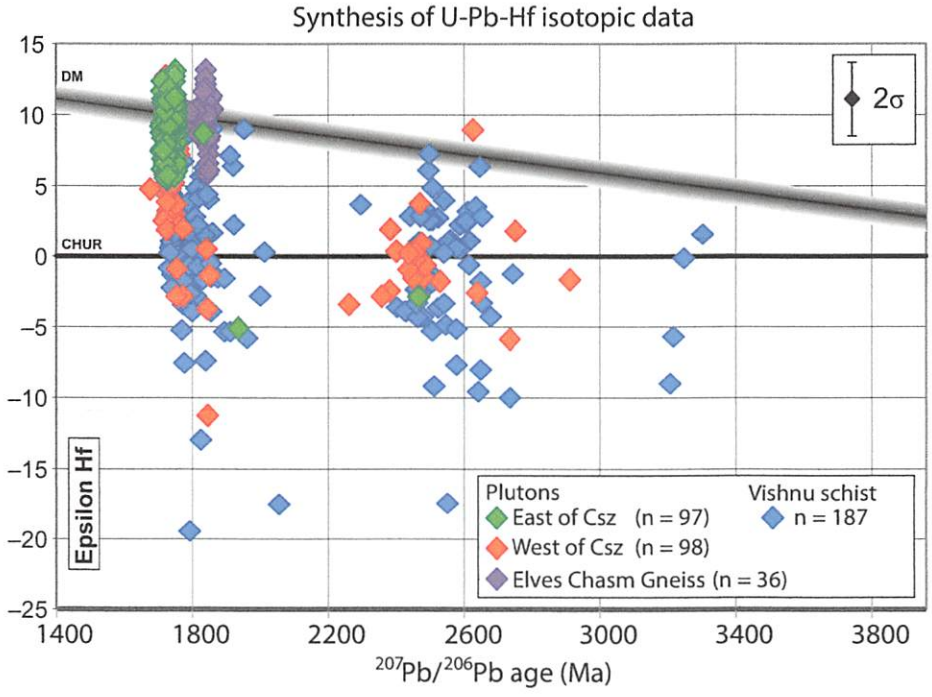

Figure 11. Synthesis of all U-Pb-Hf data from plutonic and detrital samples in Grand Canyon. Vishnu Schist is shown in blue, plutons east of the Crystal shear zone (Csz) in green, and plutons west of the Crystal shear zone in red. The dramatic difference in plutonic zircons is apparent. Paradoxically, the plutonic data suggest a suture across the shear zone, but the detrital zircon data do not. DM—depleted mantle; CHUR—chondritic uniform reservoir.

argues against a substantial Laurentian cratonic source. Mueller et al. (2011) recognized this dilemma and suggested that the Mojave Province may have evolved independently at 2.5 Ga, which was similarly proposed by Whitmeyer and Karlstrom (2007), and might seem supported by the presence of ca. 2.5 Ga lithosphere in the Mojave Province (Lee et al., 2001) and inherited zircons of the same age in plutons west of Crystal shear zone (see following).

Source of Inherited Zircons

Understanding the history of the inherited grains in the plutons is of key importance for evaluating crustal evolution models (Hawkesworth and Kemp, 2006). With the exception of the Elves Chasm basement, the plutons in Grand Canyon intrude the Vishnu Schist such that inherited grains could plausibly be assimilated from Vishnu Schist wall rocks. The similarity between U-Pb-Hf characteristics of Vishnu detrital zircons and inherited grains in plutons might suggest that this is the case. Alternatively, since petrogenetic models for granodiorites and other granitoids invoke preexisting crustal contributions by partial melting of mafic lower crust (Jung et al., 2009), assimilation and fractional crystallization (Jung et al., 2015), and/or magma mixing in the lower crust (Koteas et al., 2010), inherited grains may reflect the age of older lower-crustal igneous material similar to that representing the provenance for the metasedimentary grains. Recent models that emphasize the potential importance of sedimentary recycling via relamination (Hacker et al., 2011) allow for a hybridized possibility whereby xenocrystic grains are inherited from recycled lower crust composed of a relaminated Vishnu-like source.

Internal textures of inherited zircons as revealed by CL and BSE imaging primarily show igneous growth zoning, but textures vary even within the same pluton. The inherited cores of the Boucher pluton range from rounded and homogeneously CL-dark (K12–96.2L-1C) to almost euhedral with complex igneous zoning (K12–96.2L-17C). Similar to the Boucher pluton, the Tuna Creek pluton yielded an inherited core overgrown by a young rim (K05–100.5–1). In contrast, however, many of the inherited grains in plutons west of Crystal shear zone show no rims and range from euhedral to rounded (Fig. 9). Rounded cores or xenocrysts may suggest a detrital origin; however, partial resorption of igneous grains can yield a similar morphology. In addition, many zircons found in igneous or meta-igneous granulite-grade lower-crustal xenoliths display rounded morphologies and irregular internal textures (Hanchar and

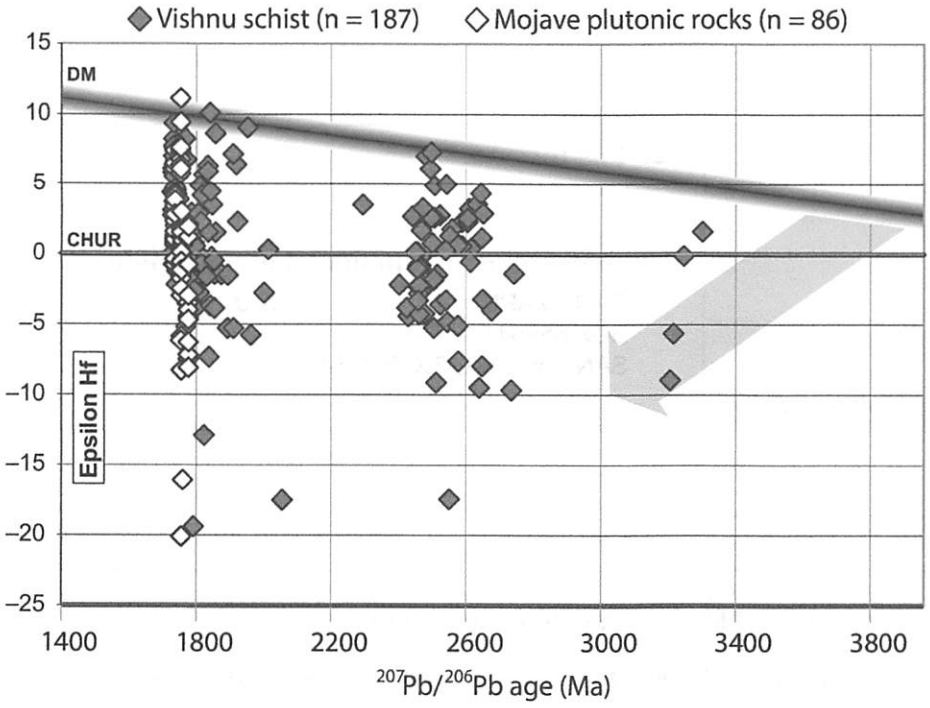

Figure 12. U-Pb-Hf isotopic data from zircons separated from 1.78 to 1.74 Ga Mojave Province plutonic rocks shown in white (Wooden et al., 2012) compared to the Vishnu Schist. DM—depleted mantle; CHUR—chondritic uniform reservoir.

Rudnick, 1995; Corfu et al., 2003; Crowley et al., 2006, 2008; Siebel et al., 2011; Sommer et al., 2013).

The varied morphology and internal texture of xenocrystic grains combined with the similarity in ages between inherited grains and the Vishnu Schist would seem to make a strong case for the assimilation of Vishnu wall rocks by plutons west of the Crystal shear zone. However, this interpretation begs the question: Why are there no inherited zircons in the plutons east of the Crystal shear zone? The Vishnu basin is uniform across the entire Grand Canyon transect; i.e., plutons on either side of the shear zone are intruding the same wall rocks. Why then, do some preserve inherited grains and not others? One explanation is that some plutons crystallized from melts that were initially undersaturated in Zr, and that any zircons assimilated from the Vishnu wall rocks were dissolved rather than preserved (Watson and Harrison, 1983; Hanchar and Watson, 2003). For example, Bickford et al. (2014) suggested that zircon saturation temperatures >850 °C might explain the dearth of inherited Paleoproterozoic zircons in Mesoproterozoic plutons across Laurentia. Although we obtained no chemical data from the samples analyzed in this study, zircon saturation temperatures for the Zoroaster, Horn, Trinity Gneiss, 96-Mile (Boucher), Tuna, Elves Chasm Gneiss, Ruby, and Diamond Creek plutons were calculated using the whole-rock major- and trace-element data presented by Babcock et al. (1979). Zircon saturation temperatures ranged from 665 °C for the Elves Chasm Gneiss to 814 °C for the Tuna Creek pluton. Given that the Tuna Creek pluton yielded the highest zircon saturation temperature, yet it preserves abundant inherited zircons, it is unlikely that zircon saturation played any role in the preservation of inherited grains. Furthermore, resorption of the older and more compositionally evolved Vishnu Schist detrital zircons would likely draw down the $\varepsilon_{Hf(t)}$ values of any zircons that ultimately crystallized from the melt, and zircons from east of the Crystal shear zone are predominantly juvenile.

In addition, even juvenile plutons display intimate field relations with Vishnu Schist (Fig. 13). While many of the plutons across the transect preserve intrusive contacts, the Zoroaster pluton in particular contains abundant screens of Vishnu Schist metaturbidites, yet it yielded no inherited zircons and a strong juvenile Hf isotopic signature.

If the xenocrystic population of zircons west of the Crystal shear zone was not derived from the Vishnu wall rocks, then it is likely that they were derived from preexisting lower crust with which juvenile arc magmas interacted. This is our preferred interpretation. The implication of this alternative source for xenocrystic grains is that west of Crystal shear zone, there is a lower-crustal substrate, perhaps variably distributed, that is substantially older than the crust currently exposed in the Grand Canyon region. The Crystal shear zone has previously been proposed as a suture between the Yavapai and Mojave Provinces, and the presence of Archean crust in the Mojave Province has been postulated (Wooden et al., 1994; Barth et al., 2000; Whitmeyer and Karlstrom, 2007; Shufeldt et al., 2010). Our data support the interpretation that the Crystal shear zone represents a discrete crustal boundary between the juvenile Yavapai Province and the more-evolved Mojave Province. Furthermore, it is our interpretation that the Mojave Province contains an older lower-crustal substrate, and that the boundary between the Mojave and Yavapai Provinces can be defined by the presence of older crust to the west of the Crystal shear zone.

Tectonic Model for Crustal Architecture

A long-standing model for the tectonic history of southwestern North America is that of successive accretion of juvenile arc terranes to the cratonic margin (Bennett and DePaolo, 1987; Karlstrom and Bowring, 1988; Whitmeyer and Karlstrom, 2007). The discovery of numerous locations that have evidence for pre–1.8 Ga crust in the orogen (Hawkins et al., 1996; Hill and Bickford, 2001; Bickford and Hill, 2007; Bickford et al., 2008), as well as substantial Archean detrital zircons in the Vishnu Schist (Shufeldt et al., 2010), highlights the need to refine plate-scale models of continental assembly (e.g., Whitmeyer and Karlstrom, 2007) by identifying the extent and character of older crust involved in the assembly of Proterozoic Laurentian terranes (Karlstrom et al., 2007). Paired analysis of metasedimentary rocks and the igneous rocks that intrude them provides unique insight into lithospheric formation in the Grand Canyon region.

We envision the Grand Canyon transect as an example of a midcrustal section of an imbricated accretionary complex. The present geometry of the transect is characterized by a strong subvertical foliation attributed to shortening during the 1.7 Ga Yavapai orogeny. The subvertical shear zones across the transect accommodated minimal vertical offset post–1.7 Ga. However, our view is that the Crystal shear zone (and perhaps others) has an earlier D_1 history and has been transposed into a D_2 orientation. Suturing happened either before or synchronously with deposition of the Vishnu Schist across both types of crust. The only pluton east of the Crystal shear

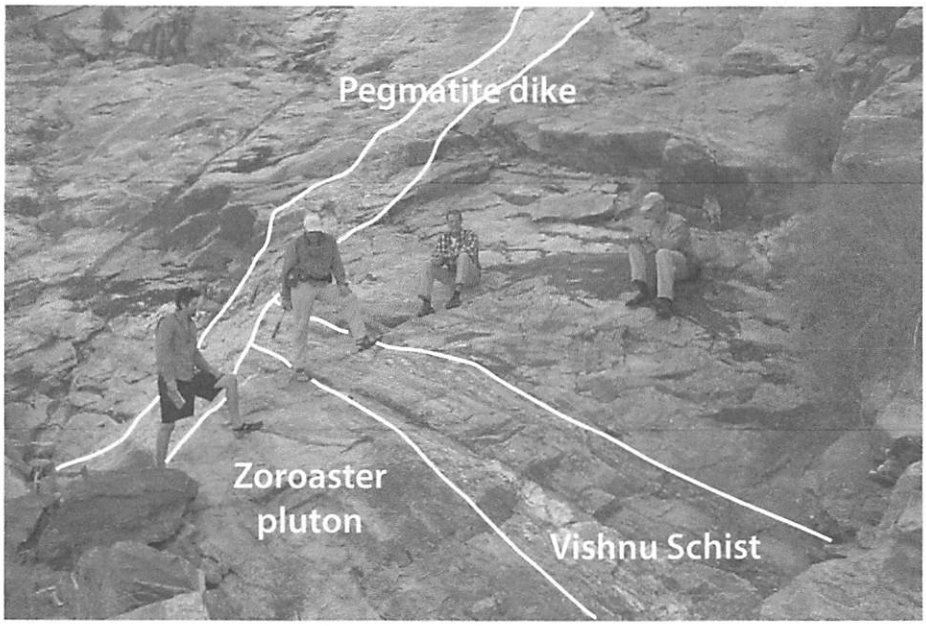

Figure 13. Field photo of the Zoroaster pluton showing one of many screens of Vishnu Schist included within the pluton.

zone to yield xenocrystic zircons is the Boucher pluton, which lies between the 96-Mile shear zone and the Crystal shear zone. The 96-Mile shear zone is shown as a minor splay of the Crystal shear zone in our cross section (Fig. 14).

Karlstrom et al. (2003) proposed that the area between the Crystal and Gneiss Canyon shear zones was an isotopically mixed boundary between the Mojave and Yavapai Provinces, analogous to the boundary in western Arizona described by Wooden and DeWitt (1991). Our sample set from the Grand Canyon includes only one pluton west of the Gneiss Canyon shear zone, the 245-Mile pluton (K06–245), which yielded xenocrystic zircons as well as juvenile values in primary grains (Fig. 9). Zircons separated from end-member Mojave plutons yielded substantially evolved $\varepsilon_{Hf(t)}$ values at 1.78–1.75 Ga (Fig. 12; Wooden et al., 2012), which are in contrast to the juvenile values of Paleoproterozoic grains from the 245-Mile pluton. While we interpret the presence of xenocrystic zircons in plutons west of the Crystal shear zone to be derived from older crustal fragments, and we suggest that the interaction of juvenile melts with these fragments gave rise to an isotopically mixed zone, the Gneiss Canyon shear zone is not the western edge of this zone. The presence of the Elves Chasm Gneiss in Mojave crust west of the Crystal shear zone provides direct evidence for the presence of older crust in the Mojave Province; however, our new data suggest that the crustal architecture is even more complex. We propose a heterogeneous crustal architecture west of the Crystal shear zone that includes: (1) juvenile 1.74 Ga crust with an inherited Archean component, (2) the juvenile 1840 Ma Elves Chasm Gneiss, and (3) fragments of Archean crust that were combined with juvenile Paleoproterozoic melts. Furthermore, we propose that these older crustal fragments increase in volume to the west, and that more extensive mixing of these fragments with Paleoproterozoic melts created the source of the inherited isotopic signature of the Mojave Province. The crustal architecture east of the Crystal shear zone appears much simpler, with predominantly juvenile 1.75 Ga crust. Eleven zircons from plutons east of the Crystal shear zone did not yield entirely juvenile $\varepsilon_{Hf(t)}$ values, which may suggest that Elves Chasm Gneiss–like crust extends further east. Our interpretations of these data reconcile the model for an isotopically mixed boundary zone between Mojave and Yavapai crust (Wooden and DeWitt, 1991; Karlstrom et al., 2003; Duebendorfer et al., 2006) with the discrete boundary at the Crystal shear zone, and they provide an explanation for the source of the characteristic evolved isotopic signature of the Mojave Province.

We propose two possible tectonic scenarios that explain the observations and that might culminate in the present geometry of the transect (Figs. 14 and 15). Deposition of the Vishnu Schist from 1750 to 1740 Ma occurred either after or during final suturing between the Mojave and Yavapai Provinces. A shallowly dipping tectonic layering (S_1) began to form shortly after deposition, likely facilitated by thrust stacking of turbidites during thickening of arc crust in the early stages of the Yavapai orogeny (Ilg et al., 1996). At close to the same time as the development of S_1, calk-alkaline granodiorite plutons intruded the Granite Gorge metamorphic suite and became imbricated within thrust sheets. The transect achieved its current configuration by the end of the Yavapai orogeny and was minimally reactivated during later Mesoproterozoic tectonism (Karlstrom et al., 1997). Deposition of the Vishnu Schist may have occurred in a trench fill sequence during final convergence between the Mojave and Yavapai Provinces (Fig. 15B). Alternatively, deposition of the Vishnu Schist may have occurred after pre–1750 Ma suturing of the Mojave and Yavapai Provinces in a back-arc basin, which was subsequently deformed and metamorphosed during the Yavapai orogeny (Fig. 15D).

CONCLUSIONS

Comparisons of metasedimentary rocks with the plutons that intrude them provide unique insight into lithospheric formation. The Grand Canyon transect is underlain by supracrustal rocks that consist of interlayered juvenile arc volcanics, and turbidites derived in part from evolved Paleoproterozoic crust of the Mojave Province, and an as-yet-undetermined Archean craton, but possibly the Gawler craton of Australia. The Vishnu Schist received little of its detritus from local Yavapai-type crust, and the Elves Chasm Gneiss did not contribute substantial detritus to the Vishnu Schist. The depositional environment of the Vishnu Schist was likely an arc setting, either a back-arc basin, or an accretionary prism in the forearc.

While the Vishnu Schist was deposited uniformly across Mojave and Yavapai crust, and does not support the existence of a crustal boundary in Grand Canyon, arc plutons yield markedly different U-Pb-Hf characteristics across the Crystal shear zone. Plutons that intrude the Vishnu Schist and serve as probes of lower-crustal melt-source regions across the entire transect are predominantly juvenile, but west of the Crystal shear zone, xenocrystic grains suggest the presence of older lower-crustal fragments, and more-evolved Paleoproterozoic grains support this conclusion.

The Paleoproterozoic rocks of the Grand Canyon are an example of a 100% exposed distributed midcrustal suture zone between the Mojave and Yavapai crustal provinces. The nature of this boundary is defined by the presence of latest Archean (ca. 2.5 Ga) lower-crustal fragments in the Mojave Province.

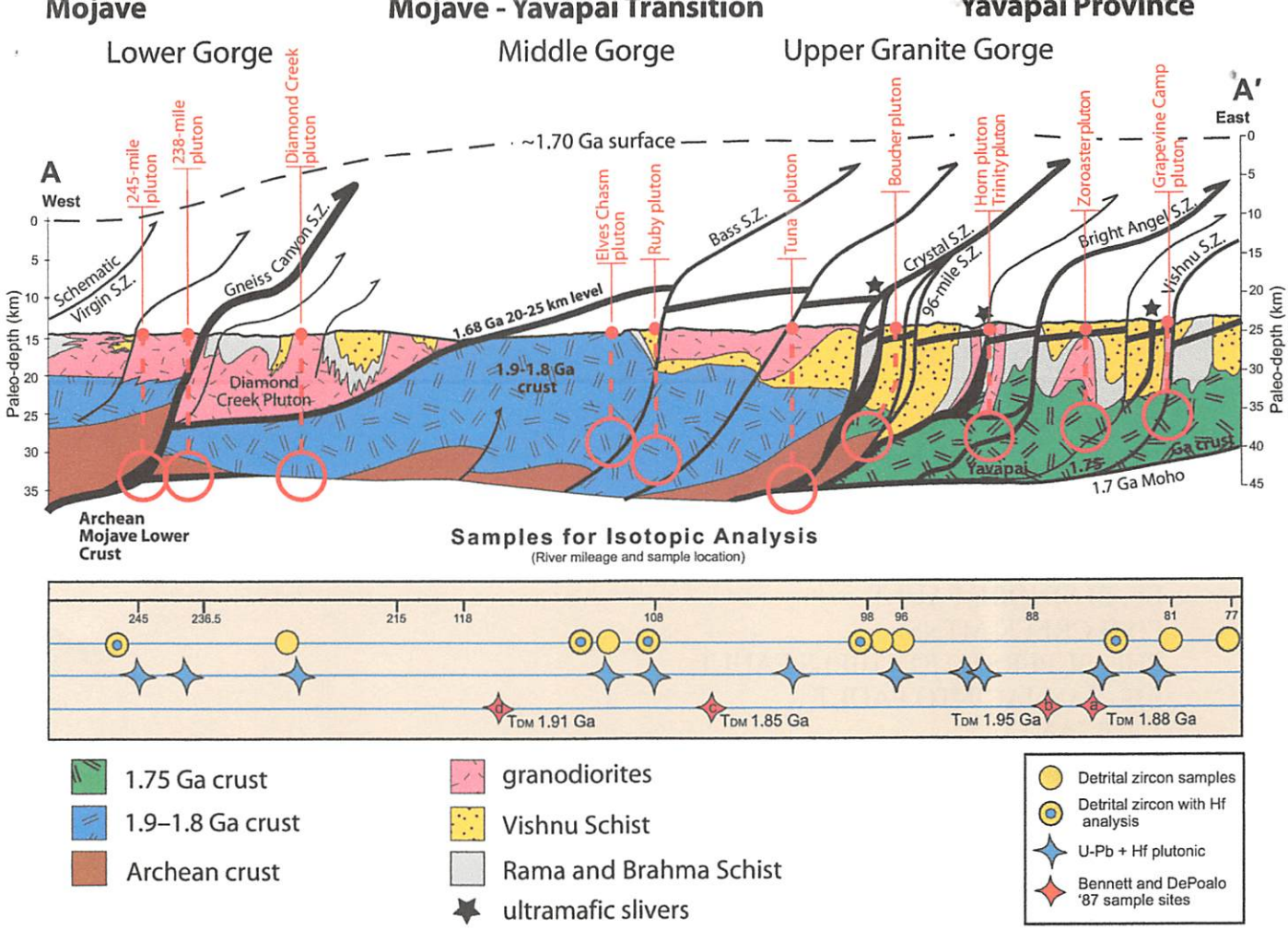

Figure 14. Schematic cross section corresponding to Figure 2A. The Grand Canyon transect is shown here as a midcrustal imbricated accretionary complex. Red circles show the concept of plutons probing their melt source regions. S.Z.—shear zone; T_{DM}—depleted mantle model age.

Figure 15 (*on following page*). Plate-tectonic cartoons illustrating possible scenarios for the depositional setting of the Vishnu Schist and lithospheric formation in the Grand Canyon region. Cartoons are drawn approximately to scale; however, crustal thickness is exaggerated. Both models meet at ca. 1740 Ma (E) when the tectonic history of the Grand Canyon region is well constrained by the work of Ilg et al. (1996), Hawkins et al. (1996), and Dumond et al. (2007). (A) Pre–1750 Ma there exists no Yavapai-type crust in the region. The Mojave arc is evolving as early as 1780 Ma. (B) Deposition of the Vishnu Schist during final convergence between the newly formed Yavapai arc and Mojave Province. Vishnu Schist is deposited across both provinces (and at least in part on the Elves Chasm Gneiss) from 1750 to 1740 Ma in a trench-fill sequence receiving most of its sediment from the Mojave Province, plus a cratonic source. (C) Alternatively, pre–1750 Ma the Yavapai and Mojave Provinces are already joined. While no >1750 Ma Yavapai crust exists in the Grand Canyon region, older Yavapai crust exists to the northeast in Colorado. (D) The Vishnu Schist is deposited across both provinces in a back-arc basin after the juxtaposition of older Yavapai crust against Mojave. (E) By 1740 Ma, the arc has migrated such that calk-alkaline plutons begin to intrude the Vishnu Schist. Thrust stacking imbricates Vishnu turbidites with arc plutons, and a shallow S_1 foliation develops. The Crystal shear zone (Csz) manifests as a boundary between Mojave and Yavapai crust. Arc plutons continue to intrude the Vishnu Schist until ca. 1710 Ma. (F) From 1710 to 1690 Ma, the transect undergoes protracted crustal shortening during the Yavapai orogeny, a penetrative subhorizontal fabric (S_2) is developed throughout the transect, and the Crystal shear zone is transposed into this orientation. The transect is intruded by crustal melts, but no longer by calk-alkaline plutons, suggesting that the arc has either migrated or terminated. By 1700 Ma, the transect resides at midcrustal levels. The box straddling the Mojave-Yavapai boundary shows the cross section of Figure 14 at 1700 Ma.

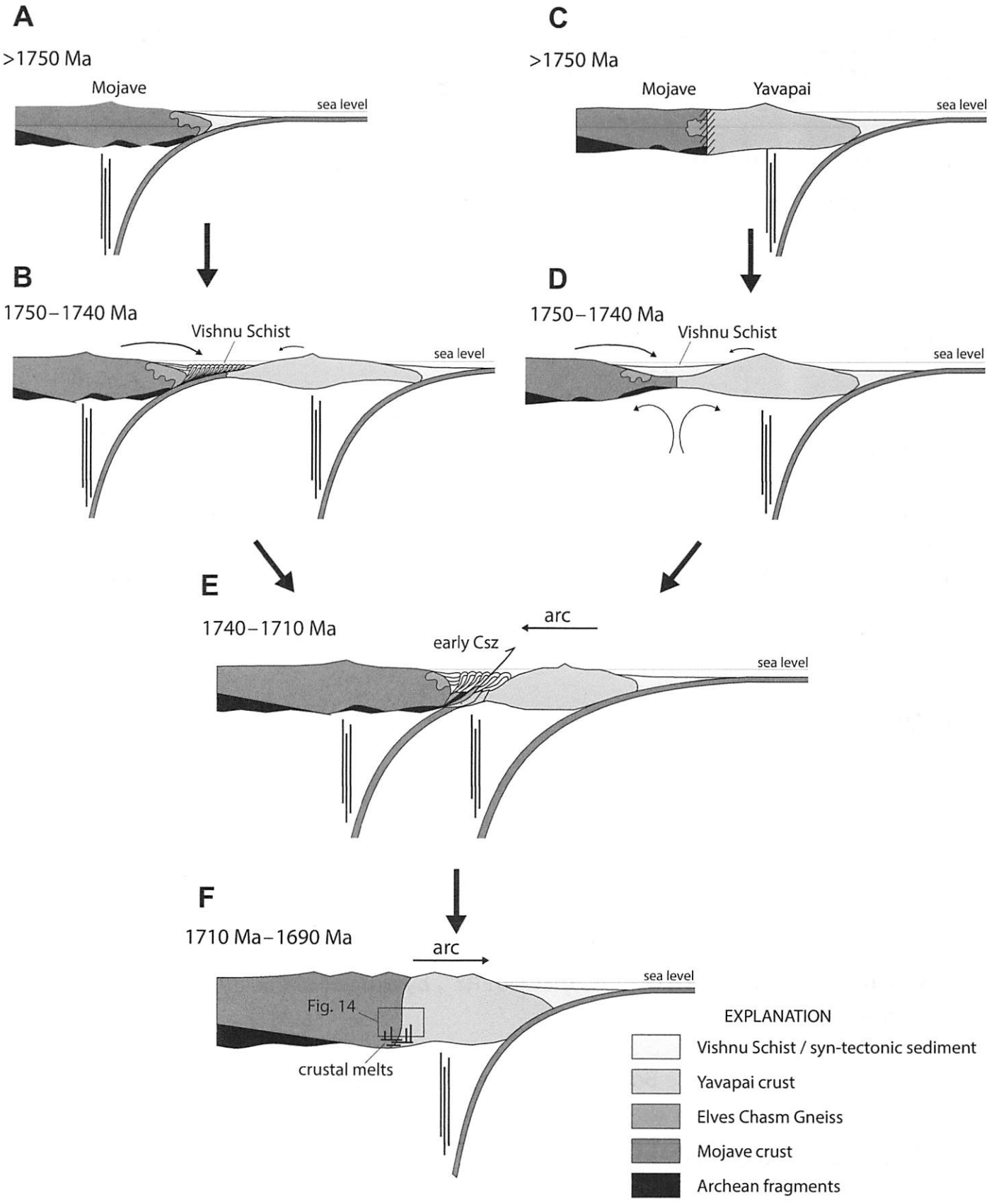
A
>1750 Ma
Mojave
sea level
C
>1750 Ma
Mojave
Yavapai
sea level
B
1750–1740 Ma
Vishnu Schist
sea level
D
1750–1740 Ma
Vishnu Schist
sea level
E
1740–1710 Ma
arc
early Csz
sea level
F
1710 Ma–1690 Ma
arc
sea level
Fig. 14
crustal melts
EXPLANATION
Vishnu Schist / syn-tectonic sediment
Yavapai crust
Elves Chasm Gneiss
Mojave crust
Archean fragments

Figure 15.

ACKNOWLEDGMENTS

This research was funded by National Science Foundation grant EAR-1145247 to Karl Karlstrom and George Gehrels. This is contribution 610 from the ARC Centre of Excellence for Core to Crust Fluid Systems (http://www.ccfs.mq.edu.au) and 998 in the GEMOC Key Centre (http://www.gemoc.mq.edu.au). Field time and sample collection was made possible by the National Park Service, Mike Timmons, and Adam Reed. Special thanks go to members of the Arizona LaserChron Center staff: Heather Alvarez, Jacobo Favela, Nicky Giesler, Mauricio Ibanez-Mejia, Clayton Loehn, Intan Yokelson, and Chelsi White. This manuscript greatly benefited from reviews by David Corrigan, David Foster, and Stephen Johnston.

REFERENCES CITED

Andersen, T., Griffin, W.L., and Pearson, N.J., 2002, Crustal evolution in the SW part of the Baltic Shield: The Hf isotope evidence: Journal of Petrology, v. 43, p. 1725–1747, doi:10.1093/petrology/43.9.1725.

Babcock, R.S., Brown, E.H., Clark, M.D., and Livingston, D.E., 1979, Geology of the older Precambrian rocks of the Grand Canyon Part II. The Zoroaster Plutonic Complex and related rocks: Precambrian Research, v. 8, p. 243–275.

Bahlburg, H., Vervoort, J.D., Andrew DuFrane, S., Carlotto, V., Reimann, C., and Cárdenas, J., 2011, The U-Pb and Hf isotope evidence of detrital zircons of the Ordovician Ollantaytambo Formation, southern Peru, and the Ordovician provenance and paleogeography of southern Peru and northern Bolivia: Journal of South American Earth Sciences, v. 32, p. 196–209, doi:10.1016/j.jsames.2011.07.002.

Barovich, K.M., Patchett, P.J., Peterman, Z.E., and Sims, P.K., 1989, Nd isotopes and the origin of 1.9–1.7 Ga Penokean continental crust of the Lake Superior region: Geological Society of America Bulletin, v. 101, p. 333–338, doi:10.1130/0016-7606(1989)101<0333.

Barth, A.P., Wooden, J.L., Coleman, D.S., and Fanning, C.M., 2000, Geochronology of the Proterozoic basement of southwesternmost North America, and the origin and evolution of the Mojave crustal province: Tectonics, v. 19, p. 616–629, doi:10.1029/1999TC001145.

Barth, A.P., Wooden, J.L., Coleman, D.S., and Vogel, M.B., 2009, Assembling and disassembling California: A zircon and monazite geochronologic framework for Proterozoic crustal evolution in southern California: The Journal of Geology, v. 117, p. 221–239, doi:10.1086/597515.

Begg, G., Griffin, W.L., O'Reilly, S.Y., and Natapov, L., 2007, Living with Archean lithosphere, *in* Spencer, J., and Titley, S., eds., Ores and Orogenesis: Circum-Pacific Tectonics, Geologic Evolution, and Ore Deposits: Arizona Geological Society Digest, v. 22, p. 44–45.

Begg, G.C., Griffin, W.L., Natapov, L.M., O'Reilly, S.Y., Grand, S., O'Neill, C.J., Hronsky, J.M.A., Poudjom Djomani, Y., Deen, T., and Bowden, P., 2009a, The lithospheric architecture of Africa: Seismic tomography, mantle petrology and tectonic evolution: Geosphere, v. 5, p. 23–50, doi:10.1130/GES00179.1.

Begg, G.C., Belousova, E.A., Griffin, W.L., O'Reilly, S.Y., and Natapov, L., 2009b, Continental versus crustal growth: Understanding the paradox: Geological Society of America Abstracts with Programs, v. 41, no. 7, p. 686.

Belousova, E.A., Griffin, W.L., Shee, S.R., Jackson, S.E., and O'Reilly, S.Y., 2001, Two age populations of zircons from the Timber Creek kimberlites, Northern Territory, as determined by laser-ablation ICP-MS analysis: Australian Journal of Earth Sciences, v. 48, p. 757–765, doi:10.1046/j.1440-0952.2001.485894.x.

Belousova, E.A., Reid, J., Griffin, W.L., and O'Reilly, S.Y., 2009, Rejuvenation vs. recycling of Archean crust in the Gawler craton, South Australia: Evidence from U-Pb and Hf isotopes in detrital zircon: Lithos, v. 113, p. 570–582, doi:10.1016/j.lithos.2009.06.028.

Belousova, E.A., Kostitsyn, Y.A., Griffin, W.L., Begg, G.C., O'Reilly, S.Y., and Pearson, N.J., 2010, The growth of the continental crust: Constraints from zircon Hf-isotope data: Lithos, v. 119, p. 457–466, doi:10.1016/j.lithos.2010.07.024.

Bennett, V.C., and DePaolo, D.J., 1987, Proterozoic crustal history of the western United States as determined by Nd mapping: Geological Society of America Bulletin, v. 99, p. 674–685, doi:10.1130/0016-7606(1987)99<674:PCHOTW>2.0.CO;2.

Bickford, M.E., and Hill, B.M., 2007, Does the arc accretion model adequately explain the Paleoproterozoic evolution of southern Laurentia?: An expanded interpretation: Geology, v. 35, p. 167, doi:10.1130/G23174A.1.

Bickford, M.E., Mueller, P.A., Kamernov, G.D., and Hill, B.M., 2008, Crustal evolution of southern Laurentia during the Paleoproterozoic: Insights from zircon Hf isotopic studies of ca. 1.75 Ga rocks in central Colorado: Geology, v. 36, p. 555–558, doi:10.1130/G24700A.1.

Bickford, M.E., Van Schmus, W.R., Karlstrom, K.E., Mueller, P.A., and Kamenov, G.D., 2014, Mesoproterozoic-trans-Laurentian magmatism: A synthesis of continent-wide age distributions, new SIMS U-Pb ages, zircon saturation temperatures, and Hf and Nd isotopic compositions: Precambrian Research (in press), doi:10.1016/j.precamres.2014.11.024.

Bouvier, A., Vervoort, J.D., and Patchett, P.J., 2008, The Lu-Hf and Sm-Nd isotopic composition of CHUR: Constraints from unequilibrated chondrites and implications for the bulk composition of terrestrial planets: Earth and Planetary Science Letters, v. 273, p. 48–57, doi:10.1016/j.epsl.2008.06.010.

Bowring, S.A., and Karlstrom, K.E., 1990, Growth, stabilization, and reactivation of Proterozoic lithosphere in the southwestern United States: Geology, v. 18, p. 1203–1206, doi:10.1130/0091-7613(1990)018<1203:GSAROP>2.3.CO;2.

Cecil, M.R., Gehrels, G., Ducea, M.N., and Patchett, P.J., 2011, U-Pb-Hf characterization of the central Coast Mountains Batholith: Implications for petrogenesis and crustal architecture: Lithosphere, v. 3, p. 247–260, doi:10.1130/L134.1.

Chamberlain, K.R., and Bowring, S.A., 1990, Proterozoic geochronologic and isotopic boundary in NW Arizona: The Journal of Geology, v. 98, p. 399–416, doi:10.1086/629412.

Corfu, F., Hanchar, J.M., Hoskin, P.W.O., and Kinny, P., 2003, Atlas of zircon textures, *in* Hanchar, J.M., and Hoskin, P.W.O., eds., Zircon: Reviews in Mineralogy and Geochemistry, v. 53, p. 469–500.

Corrigan, D., Hajnal, Z., Németh, B., and Lucas, S.B., 2005, Tectonic framework of a Paleoproterozoic arc–continent to continent–continent collisional zone, Trans-Hudson orogen, from geological and seismic reflection studies: Canadian Journal of Earth Sciences, v. 42, no. 4, p. 421–434, doi:10.1139/E05-025.

Corrigan, D., Pehrsson, S., Wodicka, N., and de Kemp, E., 2009, The Palaeoproterozoic Trans-Hudson orogen: A prototype of modern accretionary processes, *in* Murphy, J.B., Keppie, J.D., and Hynes, A.J., eds., Ancient Orogens and Modern Analogues: Geological Society of London Special Publication 327, p. 457–479, doi:10.1144/SP327.19.

Crowley, J.L., Schmitz, M.D., Bowring, S.A., Williams, M.L., and Karlstrom, K.E., 2006, U-Pb and Hf isotopic analysis of zircon in lower crustal xenoliths from the Navajo volcanic field: 1.4 Ga mafic magmatism and metamorphism beneath the Colorado Plateau: Contributions to Mineralogy and Petrology, v. 151, p. 313–330, doi:10.1007/s00410-006-0061-z.

Crowley, J.L., Brown, R.L., Gervais, F., and Gibson, H.D., 2008, Assessing inheritance of zircon and monazite in granitic rocks from the Monashee complex, Canadian Cordillera: Journal of Petrology, v. 49, p. 1915–1929, doi:10.1093/petrology/egn047.

DePaolo, D.J., 1981, Neodymium isotopes in the Colorado Front Range and crust-mantle evolution in the Proterozoic: Science, v. 291, p. 193–196.

Duebendorfer, E.M., 2007, Research focus: Crust formation in the western United States: Geology, v. 35, no. 2, p. 191, doi:10.1130/0091-7613(2007)35[191:RFCFIT]2.0.CO;2.

Duebendorfer, E.M., Chamberlain, K.R., and Fry, B., 2006, Mojave-Yavapai boundary zone, southwestern United States: A rifting model for the formation of an isotopically mixed crustal boundary zone: Geology, v. 34, p. 681–684, doi:10.1130/G22581.1.

Dumond, G., Mahan, K.H., Williams, M.L., and Karlstrom, K.E., 2007, Crustal segmentation, composite looping pressure-temperature paths, and magma-enhanced metamorphic field gradients: Upper Granite Gorge, Grand Canyon, USA: Geological Society of America Bulletin, v. 119, p. 202–220, doi:10.1130/B25903.1.

Elston, D.P., 1989, Grand Canyon Supergroup, northern Arizona: Stratigraphic summary and preliminary paleomagnetic correlations with parts of other North American Proterozoic successions, *in* Jenney, J.P., and Reynolds, S.J., eds., Geologic Evolution of Arizona: Arizona Geological Society Digest, v. 17, p. 259–272.

Farmer, G.L., and DePaolo, D.J., 1983, Origin of Mesozoic and Tertiary granite in the western United States and implications for Pre-Mesozoic crustal structure: 1. Nd and Sr isotopic studies in the geocline of the northern Great Basin: Journal of Geophysical Research, v. 88, p. 3379, doi:10.1029/JB088iB04p03379.

Finger, F., 1997, Variscan granitoids of central Europe: Their typology, potential sources and tectonothermal relations: Mineralogy and Petrology, v. 61, p. 67–96, doi:10.1007/BF01172478.

Foster, D.A., Mueller, P.A., Heatherington, A., Gifford, J.N., and Kalakay, T.J., 2012, Lu-Hf systematics of magmatic zircons reveal a Proterozoic crustal boundary under the Cretaceous Pioneer batholith, Montana: Lithos, v. 142–143, p. 216–225, doi:10.1016/j.lithos.2012.03.005.

Friedman, R.M., Mahoney, J.B., and Cui, Y., 1995, Magmatic evolution of the southern Coast Belt: Constraints from Nd-Sr isotopic systematics and geochronology of the southern Coast plutonic complex: Canadian Journal of Earth Sciences, v. 32, p. 1681–1698, doi:10.1139/e95-133.

Gehrels, G., and Pecha, M., 2014, Detrital zircon U-Pb geochronology and Hf isotope geochemistry of Paleozoic and Triassic passive margin strata of western North America: Geosphere, v. 10, p. 49–65, doi:10.1130/GES00889.1.

Gehrels, G.E., Valencia, V., and Pullen, A., 2006, Detrital zircon geochronology by laser-ablation multicollector ICPMS at the Arizona LaserChron Center, *in* Loszewski, T., and Huff, W., eds., Geochronology: Emerging Opportunities: Paleontology Society Short Course: Paleontology Society Papers, v. 11, 10 p.

Gehrels, G.E., Valencia, V.A., and Ruiz, J., 2008, Enhanced precision, accuracy, efficiency, and spatial resolution of U-Pb ages by laser ablation–multicollector–inductively coupled plasma–mass spectrometry: Geochemistry, Geophysics, Geosystems, v. 9, Q03017, doi:10.1029/2007GC001805.

Gonzales, D.A., and Van Schmus, W.R., 2007, Proterozoic history and crustal evolution in southwestern Colorado: Insight from U/Pb and Sm/Nd data: Precambrian Research, v. 154, p. 31–70, doi:10.1016/j.precamres.2006.12.001.

Griffin, W.L., Pearson, N.J., Belousova, E., Jackson, S.E., O'Reilly, S.Y., van Achterberg, E., and Shee, S.R., 2000, The Hf isotope composition of cratonic mantle: LAM-MC-ICPMS analysis of zircon megacrysts in kimberlites: Geochimica et Cosmochimica Acta, v. 64, p. 133–147, doi:10.1016/S0016-7037(99)00343-9.

Griffin, W.L., Wang, X., Jackson, S., Pearson, N., O'Reilly, S.Y., Xu, X., and Zhou, X., 2002, Zircon chemistry and magma mixing, SE China: In-situ analysis of Hf isotopes, Tonglu and Pingtan igneous complexes: Lithos, v. 61, p. 237–269, doi:10.1016/S0024-4937(02)00082-8.

Griffin, W.L., Belousova, E.A., Shee, S.R., Pearson, N.J., and O'Reilly, S.Y., 2004, Archean crustal evolution in the northern Yilgarn craton: U-Pb and Hf-isotope evidence from detrital zircons: Precambrian Research, v. 131, p. 231–282, doi:10.1016/j.precamres.2003.12.011.

Griffin, W.L., O'Reilly, S.Y., Afonso, J.C., and Begg, G.C., 2008, The composition and evolution of lithospheric mantle: A re-evaluation and its tectonic implications: Journal of Petrology, v. 50, p. 1185–1204, doi:10.1093/petrology/egn033.

Griffin, W.L., Begg, G.C., Dunn, D., O'Reilly, S.Y., Natapov, L.M., and Karlstrom, K., 2011, Archean lithospheric mantle beneath Arkansas: Continental growth by microcontinent accretion: Geological Society of America Bulletin, v. 123, no. 9–10, p. 1763–1775, doi:10.1130/B30253.1.

Hacker, B.R., Kelemen, P.B., and Behn, M.D., 2011, Differentiation of the continental crust by relamination: Earth and Planetary Science Letters, v. 307, p. 501–516, doi:10.1016/j.epsl.2011.05.024.

Hanchar, J.M., and Rudnick, R.L., 1995, Revealing hidden structures, the application of CL and BSE imaging to dating zircons from lower crustal xenoliths: Lithos, v. 36, p. 289–303, doi:10.1016/0024-4937(95)00022-4.

Hanchar, J.M., and Watson, E.B., 2003, Zircon saturation thermometry, *in* Hanchar, J.M., and Hoskin, P.W.O., eds., Zircon: Reviews in Mineralogy and Geochemistry, v. 53, p. 89–112.

Hawkesworth, C.J., and Kemp, I.S., 2006, Using hafnium and oxygen isotopes in zircons to unravel the record of crustal evolution: Chemical Geology, v. 226, p. 144–162, doi:10.1016/j.chemgeo.2005.09.018.

Hawkins, D.P., 1996, U-Pb Geochronological Constraints on the Tectonic and Thermal Evolution of Paleoproterozoic Crust in the Grand Canyon, Arizona [Ph.D. thesis]: Cambridge, Massachusetts Institute of Technology, 320 p.

Hawkins, D.P., Bowring, S.A., Ilg, B.R., Karlstrom, K.E., and Williams, M.L., 1996, U-Pb geochronologic constraints on the Paleoproterozoic crustal evolution of the Upper Granite Gorge, Grand Canyon, Arizona: Geological Society of America Bulletin, v. 108, p. 1167–1181, doi:10.1130/0016-7606(1996)108<1167:UPGCOT>2.3.CO;2.

Hill, B.M., and Bickford, M.E., 2001, Paleoproterozoic rocks of central Colorado: Accreted arcs or extended older crust?: Geology, v. 29, p. 1015–1018, doi:10.1130/0091-7613(2001)029<1015:PROCCA>2.0.CO;2.

Hoffman, P.F., 1988, United plates of America, and growth of Laurentia: American Journal of Science, v. 16, p. 543–603.

Huntoon, P.W., Billingsley, G.H., Jr., Breed, W.J., Sears, J.W., Ford, T.D., Clark, M.D., Babcock, R.S., and Brown, E.H., 1980, Geologic Map of the Eastern Part of the Grand Canyon National Park: Grand Canyon, Arizona, Grand Canyon Natural History Association, scale 1:62,500.

Ilg, B.R., Karlstrom, K.E., Hawkins, D.P., and Williams, M.L., 1996, Tectonic evolution of Paleoproterozoic rocks in the Grand Canyon: Insights into middle-crustal processes: Geological Society of America Bulletin, v. 108, p. 1149–1166, doi:10.1130/0016-7606(1996)108<1149.

Iriondo, A., Premo, W.R., Martinex-Torres, L.M., Budahn, J.R., Atkinson, W.W., Jr., Siems, D.F., and Guaras-Gonzalez, B., 2004, Isotopic, geochemical, and temporal characterization of Proterozoic basement rocks in the Quitovac region, northwestern Sonora, Mexico: Implications for the reconstruction of the southwestern margin of Laurentia: Geological Society of America Bulletin, v. 116, p. 154–170, doi:10.1130/B25138.1.

Jackson, S.E., Pearson, N.J., Griffin, W.L., and Belousova, E.A., 2004, The application of laser ablation–inductively coupled plasma–mass spectrometry to in situ U-Pb zircon geochronology: Chemical Geology, v. 211, p. 47–69, doi:10.1016/j.chemgeo.2004.06.017.

Jahn, B., Wu, F., and Chen, B., 2000, Granitoids of the Central Asian Orogenic Belt and continental growth in the Phanerozoic, *in* Barbarin, B., Stephens, W.E., Bonin, B., Bouchez, J.-L., Clarke, D.B., Cuney, M., and Martin, H., eds., The Fourth Hutton Symposium on the Origin of Granites and Related Rocks: Geological Society of America Special Paper 350, p. 181–193, doi:10.1130/0-8137-2350-7.181.

Jones, D.S., Barnes, C.G., Premo, W.R., and Snoke, A.W., 2011, The geochemistry and petrogenesis of the Paleoproterozoic Green Mountain arc: A composite(?), bimodal, oceanic, fringing arc: Precambrian Research, v. 185, p. 231–249, doi:10.1016/j.precamres.2011.01.011.

Jung, S., Masberg, P., Mihm, D., and Hoernes, S., 2009, Partial melting of diverse crustal sources—Constraints from Sr-Nd-O isotope compositions of quartz diorite–granodiorite–leucogranite associations (Kaoko belt, Namibia): Lithos, v. 111, p. 236–251, doi:10.1016/j.lithos.2008.10.010.

Jung, S., Kröner, A., Hauff, F., and Masberg, P., 2015, Petrogenesis of synorogenic diorite-granodiorite-granite complexes in the Damara belt, Namibia: Constraints from U-Pb zircon ages and Sr-Nd-Pb isotopes: Journal of African Earth Sciences, v. 101, p. 253–265, doi:10.1016/j.jafrearsci.2014.09.015.

Karlstrom, K.E., and Bowring, S.A., 1988, Early Proterozoic assembly of tectonostratigraphic terranes in southwestern North America: The Journal of Geology, v. 96, p. 561–576, doi:10.1086/629252.

Karlstrom, K.E., and Bowring, S.A., 1993, Proterozoic orogenic history of Arizona, *in* Reed, J.C., et al., eds., Precambrian: Conterminous U.S.: Boulder, Colorado, Geological Society of America, Geology of North America, v. C-2, p. 188–211.

Karlstrom, K.E., Heizler, M.T., and Williams, M.L., 1997, ^{40}Ar-^{39}Ar muscovite thermochronology within the Upper Granite Gorge of the Grand Canyon: Eos (Transactions, American Geophysical Union), v. 78, no. 46, Fall Meeting supplement, p. F784.

Karlstrom, K.E., Ilg, B.R., Williams, M.L., Hawkins, D.P., Bowring, S.A., and Seaman, J.S., 2003, Paleoproterozoic rocks of the Granite Gorges, *in* Bues, S.S., and Morales, M., eds., Grand Canyon Geology: New York, Oxford University Press, p. 9–38.

Karlstrom, K.E., Amato, J.M., Williams, M.L., Heizler, M., Shaw, C.A., Read, A.S., and Bauer, P., 2004, Proterozoic tectonic evolution of the New Mexico region: A synthesis, *in* Mack, G.H., and Giles, K.A., eds., The Geology of New Mexico: A Geologic History: Socorro, New Mexico, New Mexico Geological Society, p. 1–34.

Karlstrom, K.E., Whitmeyer, S.J., Williams, M.L., Bowring, S.A, and Jessup, M.J., 2007, Does the arc-accretion model adequately explain the Paleoproterozoic evolution of southern Laurentia: An expanded interpretation: Comment and Reply: Comment: Geology, v. 35, p. e143–e144, doi:10.1130/G23971C.1.

Kohút, M., and Nabelek, P.I., 2008, Geochemical and isotopic (Sr, Nd and O) constraints on sources for Variscan granites in the Western Carpathians—Implications for crustal structure and tectonics: Journal of Geosciences (Prague), v. 53, p. 307–322, doi:10.3190/jgeosci.033.

Koteas, G.C., Williams, M.L., Seaman, S.J., and Dumond, G., 2010, Granite genesis and mafic-felsic magma interaction in the lower crust: Geology, v. 38, p. 1067–1070, doi:10.1130/G31017.1.

Kovalenko, V.I., Yarmolyuk, V.V., Kovach, V.P., Kotov, A.B., Kozakov, I.K., Salnikova, E.B., and Larin, A.M., 2004, Isotope provinces, mechanisms of generation and sources of the continental crust in the Central Asian mobile belt: Geological and isotopic evidence: Journal of Asian Earth Sciences, v. 23, p. 605–627, doi:10.1016/S1367-9120(03)00130-5.

Lee, C.T., Yin, Q., Rudnick, R.L., and Jacobsen, S.B., 2001, Preservation of ancient and fertile lithospheric mantle beneath the southwestern United States: Nature, v. 411, p. 69–73, doi:10.1038/35075048.

Mueller, P.A., Wooden, J.L., Mogk, D.W., and Foster, D.A., 2011, Paleoproterozoic evolution of the Farmington zone: Implications for terrane accretion in southwestern Laurentia: Lithosphere, v. 3, p. 401–408, doi:10.1130/L161.1.

Ramo, O.T., and Calzia, J.P., 1998, Nd isotopic composition of cratonic rocks in the southern Death Valley region; evidence for a substantial Archean source component in Mojavia: Geology, v. 26, p. 891–894, doi:10.1130/0091-7613(1998)026<0891:NICOCR>2.3.CO;2.

Reymer, A., and Schubert, G., 1986, Rapid growth of some major segments of continental crust: Geology, v. 14, p. 299–302, doi:10.1130/0091-7613(1986)14<299:RGOSMS>2.0.CO;2.

Samson, S.D., McClelland, W.C., Patchett, P.J., Gehrels, G.E., and Anderson, R.G., 1989, Evidence from neodymium isotopes for mantle contributions to Phanerozoic crustal genesis in the Canadian Cordillera: Nature, v. 337, p. 705–709, doi:10.1038/337705a0.

Samson, S.D., Patchett, P.J., McClelland, W.C., and Gehrels, G.E., 1991, Nd isotopic characterization of metamorphic rocks in the Coast Mountains, Alaskan and Canadian Cordillera: Ancient crust bounded by juvenile terranes: Tectonics, v. 10, p. 770–780, doi:10.1029/90TC02732.

Seaman, S.J., Karlstrom, K.E., Williams, M.L., and Petruski, A.J.. 1997, Proterozoic ultramafic bodies in the Grand Canyon: Geological Society of America Abstracts with Programs, v. 29, no. 6, p. A-89.

Shufeldt, O.P., Karlstrom, K.E., Gehrels, G.E., and Howard, K.E., 2010, Archean detrital zircons in the Proterozoic Vishnu Schist of the Grand Canyon, Arizona: Implications for crustal architecture and Nuna supercontinent reconstructions: Geology, v. 38, p. 1099–1102, doi:10.1130/G31335.1.

Siebel, W., Shang, C.K., Thern, E., Danišík, M., and Rohrmüller, J., 2011, Zircon response to high-grade metamorphism as revealed by U-Pb and cathodoluminescence studies: International Journal of Earth Sciences, v. 101, p. 2105–2123, doi:10.1007/s00531-012-0772-5.

Sommer, H., Wan, Y., Kroner, A., Xie, H., and Jacob, D.E., 2013, Shrimp zircon ages and petrology of lower crustal granulite xenoliths from the Letseng-La-Terae Kimberlite, Lesotho: Further evidence for a Namaqua-Natal connection: South African Journal of Geology, v. 116, p. 183–198, doi:10.2113/gssajg.116.2.183.

Strickland, A., Wooden, J.L., Mattinson, C.G., Ushikubo, T., Miller, D.M., and Valley, J.W., 2012, Proterozoic evolution of the Mojave crustal province as preserved in the Ivanpah Mountains, southeastern California: Precambrian Research, v. 224, p. 222–241, doi:10.1016/j.precamres.2012.09.006.

Vervoort, J.D., and Blichert-Toft, J., 1999, Evolution of the depleted mantle: Hf isotope evidence from juvenile rocks through time: Geochimica et Cosmochimica Acta, v. 63, p. 533–556.

Vervoort, J.D., Patchett, P.J., Blichert-Toft, J., and Albare, F., 1999, Relationships between Lu-Hf and Sm-Nd isotopic systems in the global sedimentary system: Earth and Planetary Science Letters, v. 168, p. 79–99, doi:10.1016/S0012-821X(99)00047-3.

Voice, P.J., Kowalewski, M., and Eriksson, K.A., 2011, Quantifying the timing and rate of crustal evolution: Global compilation of radiometrically dated detrital zircon grains: The Journal of Geology, v. 119, p. 109–126, doi:10.1086/658295.

Watson, E.B., and Harrison, T.M., 1983, Zircon saturation revisited: Temperature and compositional effects in a variety of crustal magma types: Earth and Planetary Science Letters, v. 64, p. 295–304, doi:10.1016/0012-821X(83)90211-X.

Whitmeyer, S.J., and Karlstrom, K.E., 2007, Tectonic model for the Proterozoic growth of North America: Geosphere, v. 3, p. 220–259, doi:10.1130/GES00055.1.

Windley, B.F., 2003, Continental growth in the Proterozoic: A global perspective, *in* Yoshida, M., Windley, B.E., and Dasgupta, S., eds., Proterozoic East Gondwana: Supercontinent Assembly and Breakup: Geological Society of London Special Publication 206, p. 23–33, doi:10.1144/GSL.SP.2003.206.01.03.

Wooden, J.L., and DeWitt, E., 1991, Pb isotopic evidence for the boundary between the Early Proterozoic Mojave and central Arizona crustal provinces in western Arizona: Arizona Geological Society Digest, v. 19, p. 27–50.

Wooden, J.L., and Miller, D.M., 1990, Chronologic and isotopic framework for early Proterozoic crustal evolution in the eastern Mojave Desert region, SE California: Journal of Geophysical Research, v. 95, p. 20,133–20,146, doi:10.1029/JB095iB12p20133.

Wooden, J.L., Nutman, A.P., Howard, K.A., Bryant, B., DeWitt, E., and Mueller, P.A., 1994, Shrimp U-Pb zircon evidence for Late Archean and Early Proterozoic crustal evolution in the Mojave province and central Arizona crustal provinces [abs.]: Geological Society of America Abstracts with Programs, v. 26, no. 6, p. 69.

Wooden, J.L., Barth, P., and Mueller, P.A., 2012, Crustal growth and tectonic evolution of the Mojave crustal province: Insights from hafnium isotope systematics in zircons: Lithosphere, v. 5, p. 17–28, doi:10.1130/L218.1.

Science Editor: David Ian Schofield
Associate Editor: Stephen T. Johnston

Manuscript Received 31 October 2014
Revised Manuscript Received 5 February 2015
Manuscript Accepted 16 March 2015

Printed in the USA